AMERICAN SOCIETY FOR MICROBIOLOGY | Journal of Virology®

STRUCTURE AND ASSEMBLY

Autographa californica Nucleopolyhedrovirus AC141 (Exon0), a Potential E3 Ubiquitin Ligase, Interacts with Viral Ubiquitin and AC66 To Facilitate Nucleocapsid Egress

Siddhartha Biswas,[a] Leslie G. Willis,[b] Minggang Fang,[b] Yingchao Nie,[b] David A. Theilmann[a,b]

[a]Plant Science, Faculty of Land Food Systems, University of British Columbia, Vancouver, BC, Canada

[b]Summerland Research and Development Center, Agriculture and Agri-Food Canada, Summerland, BC, Canada

ABSTRACT During the infection cycle of Autographa californica multiple nucleopolyhedrovirus (AcMNPV), two forms of virions are produced, budded virus (BV) and occlusion-derived virus (ODV). Nucleocapsids that form BV have to egress from the nucleus, whereas nucleocapsids that form ODV remain inside the nucleus. The molecular mechanism that determines whether nucleocapsids remain inside or egress from the nucleus is unknown. AC141 (a predicted E3 ubiquitin ligase) and viral ubiquitin (vUbi) have both been shown to be required for efficient BV production. In this study, it was hypothesized that vUbi interacts with AC141, and in addition, that this interaction was required for BV production. Deletion of both *ac141* and *vubi* restricted viral infection to a single cell, and BV production was completely eliminated. AC141 was ubiquitinated by either vUbi or cellular Ubi, and this interaction was required for optimal BV production. Nucleocapsids in BV, but not ODV, were shown to be specifically ubiquitinated by vUbi, including a 100-kDa protein, as well as high-molecular-weight conjugates. The viral ubiquitinated 100-kDa BV-specific nucleocapsid protein was identified as AC66, which is known to be required for BV production and was shown by coimmunoprecipitation and mass spectrometry to interact with AC141. Confocal microscopy also showed that AC141, AC66, and vUbi interact at the nuclear periphery. These results suggest that ubiquitination of nucleocapsid proteins by vUbi functions as a signal to determine if a nucleocapsid will egress from the nucleus and form BV or remain in the nucleus to form ODV.

IMPORTANCE Baculoviruses produce two types of virions called occlusion-derived virus (ODV) and budded virus (BV). ODVs are required for oral infection, whereas BV enables the systemic spread of virus to all host tissues, which is critical for killing insects. One of the important steps for BV production is the export of nucleocapsids out of the nucleus. This study investigated the molecular mechanisms that enable the selection of nucleocapsids for nuclear export instead of being retained within the nucleus, where they would become ODV. Our data show that ubiquitination, a universal cellular process, specifically tags nucleocapsids of BV, but not those found in ODV, using a virus-encoded ubiquitin (vUbi). Therefore, ubiquitination may be the molecular signal that determines if a nucleocapsid is destined to form a BV, thus ensuring lethal infection of the host.

KEYWORDS AcMNPV, AC141, RING motif, viral ubiquitin, cellular ubiquitin, budded virus (BV), occlusion-derived virus (ODV), nucleocapsids, AC66, VP80, ubiquitination

Autographa californica multiple nucleopolyhedrovirus (AcMNPV) has a large double-stranded DNA genome that is packaged into rod-shaped nucleocapsids, which are utilized to form two types of virions, budded virus (BV) and occlusion-derived virus (ODV). During the late stage of infection, new nucleocapsids are synthesized in the

Received 6 October 2017 **Accepted** 8 November 2017

Accepted manuscript posted online 15 November 2017

Citation Biswas S, Willis LG, Fang M, Nie Y, Theilmann DA. 2018. Autographa californica nucleopolyhedrovirus AC141 (Exon0), a potential E3 ubiquitin ligase, interacts with viral ubiquitin and AC66 to facilitate nucleocapsid egress. J Virol 92:e01713-17. https://doi.org/10.1128/JVI.01713-17.

Editor Rozanne M. Sandri-Goldin, University of California, Irvine

© Crown copyright 2018. The government of Australia, Canada, or the UK ("the Crown") owns the copyright interests of authors who are government employees. The Crown Copyright is not transferable.

Address correspondence to David A. Theilmann, david.theilmann@agr.gc.ca.

nuclear virogenic stroma, followed by transport to the ring zone at the nuclear periphery. Nucleocapsids destined to become BV egress from the nucleus and traverse through the cytoplasm to the plasma membrane, from where they bud to form BV. During the late and very late phases of infection, nucleocapsids that are retained inside the nucleus form ODV. BV obtains its envelope by budding from the plasma membrane, whereas the ODV envelope is derived from the inner nuclear membrane (1). The function of BV is to mediate the systemic spread of viral infection between insect tissues, whereas ODVs are utilized for interhost transmission and are specifically required for initiating the infection of the insect by binding to the midgut epithelial cells. The mechanism by which nucleocapsids are designated to become BV or ODV is unknown, but some form of signaling to enable the differential trafficking is assumed to occur.

A wide variety of cellular processes, including trafficking, are regulated by post-translational modifications of proteins by ubiquitin (Ubi) (2–4). The ubiquitination pathway initiates with a thiol-ester linkage between ubiquitin-activating E1 enzymes and the C-terminal glycine of ubiquitin. The activated ubiquitin is transferred to a ubiquitin-conjugating E2 enzyme. The transfer of ubiquitin from E2 to a substrate is catalyzed by E3 ubiquitin ligases (2, 5, 6). Substrate specificity for ubiquitination is determined by the E3 ubiquitin ligases, which is why mammals have hundreds of E3 proteins but only approximately 35 E2s and two E1s (5, 7, 8). E3 enzymes are classified into three families according to their structures and functions: (i) the homologous to E6AP C-terminus (HECT) domain family, (ii) the really interesting new gene (RING) domain family, and (iii) the RING-between-RING (RBR) domain family (7, 8). Many studies have shown that viruses utilize the host ubiquitination system at different stages of the infection cycle, but they are also known to either encode their own E3 ubiquitin ligases or encode adapter proteins that recruit the cellular E3 ligases (9, 10).

AC141 (also known as Exon0) is a nucleocapsid-associated protein expressed at late times postinfection (p.i.) and is specifically required for BV production (11). Deletion of *ac141* reduces BV production by more than 99.99%, and nucleocapsids are not able to egress from the nucleus (11, 12). AC141 contains a C-terminal RING domain that is homologous to those found in E3 ubiquitin ligases, and deletion analysis has shown it is required for optimal BV production (13). The predicted RING motif of AC141 is conserved among sequenced genomes of alphabaculoviruses that infect lepidoptera (11). The consensus sequence of the AC141 RING motif, $C_3C(Y/F)C_4$, is different from the C_3HC_4 motif of most other cellular or AcMNPV RING domain proteins (11). A tyrosine or phenylalanine replaces histidine, and there is an additional conserved cysteine residue adjacent to the third cysteine. The RING motif binds two zinc atoms in a cross-brace finger configuration and is required for interaction with E2 enzymes (14).

Ubiquitin is a small, 76-amino-acid (aa) protein that is present in cells either in a free form or covalently attached to other proteins. Ubiquitin can be linked to one lysine or to the multiple lysine residues of a substrate, resulting in mono- or multiubiquitination, respectively. Ubiquitin also has intrinsic lysine residues that can be used to form polyubiquitin chains (3, 15). Polyubiquitin chains, linked to the various ubiquitin lysines, are required for different cellular processes. For example, attachment of K48 polyubiquitin chains to substrate proteins is a signal for degradation via the 26S proteasome-mediated pathway (3, 15, 16). K63-linked polyubiquitination of proteins is a signal for protein trafficking or for a DNA damage response (15, 16). Baculoviruses are a unique group of viruses, as they encode their own ubiquitin (*vubi*). AcMNPV viral ubiquitin (vUbi) is 77 amino acids long and has 76% amino acid identity with cellular ubiquitin (cUbi) (17). All the cUbi lysine residues are conserved, but vUbi also has an extra lysine residue at position 54. Analysis of *vubi* has shown that it is expressed as a late gene, and disruption by a frameshift mutation did not have any impact on virus replication; however, BV production was reduced 5- to 10-fold (18, 19). Biochemical analysis has shown that both cUbi and vUbi are attached to the inner side of the BV envelope via a phospholipid anchor (20). In *in vitro* ubiquitination assays using mammalian E1, E2, and E3 enzymes, vUbi was found to be less efficient than cUbi in supporting ATP-

dependent proteolysis. vUbi and cUbi were functionally indistinguishable in the E1 and E2 steps of ubiquitin conjugation. However, the rate of transfer by the mammalian E3 ubiquitin ligase of vUbi to a substrate was significantly lower than for cUbi (21). Thus, the transfer of vUbi to a substrate might require a different E3 ligase or a different mechanism of interaction between E3 ligase and an E2 conjugated with vUbi.

In addition to AC141, the AcMNPV regulatory proteins IE2, PE38, IAP1, and IAP2 all contain classic cellular C3HC4 RING motifs and have been shown, or predicted, to be E3 ligases (22–25). The AC141 RING motif, as indicated above, has conserved differences compared to cellular E3 proteins. As both AC141 and vUbi are required for BV production, we hypothesized that AC141 is a potential ubiquitin E3 ligase that specifically interacts with vUbi, as opposed to cUbi, and that this activity is required for optimal BV production. The results described in this study show that AC141 and vUbi interact and the deletion of both *ac141* and *vubi* eliminates BV production. In addition, BV nucleocapsids were found to be highly ubiquitinated by vUbi compared to ODV nucleocapsids. We also demonstrate that the nucleocapsid protein AC66 associates with vUbi and AC141 and that this interaction suggests a mechanism by which nucleocapsids are designated for nuclear egress and subsequent BV formation.

RESULTS

BV production of *ac141* and *vubi* single- and double-gene-knockout viruses. To study the interaction between AC141 and vUbi, a series of single- and double-gene-knockout (KO) viruses were constructed in which *ac141*, *vubi*, or both genes were deleted, followed by repair with either one or both genes. The *ac141* and *vubi* repair genes included sequences for either C-terminal hemagglutinin (HA) or Myc epitope tags, respectively. These viruses were named *ac141*KO, *vubi*KO, *vubi*KO-Myc-*vubi*, *ac141*+*vubi*2×KO, 2×KO-HA-*ac141*+Myc-*vubi*, 2×KO-HA-*ac141*, and 2×KO-Myc-*vubi* (Fig. 1A and Table 1). To determine and compare the impacts of deleting either one or both of the *ac141* and *vubi* genes, time course experiments were conducted to analyze BV production. Cells were transfected with purified bacmids from the above-mentioned viruses. In addition, a control transfection of a *gp64* deletion virus that is unable to produce BV was also performed (26–28). The *ac141*KO repair virus, *ac141*KO-HA-*ac141*, was not used in this experiment, as it has been previously analyzed and has been shown to be equivalent to the wild type (WT) (11, 13, 29). BV production of 2×KO-HA-*ac141*+Myc-*vubi* and *vubi*KO-Myc-*vubi* were equivalent to that of the WT at 24, 48, 72, and 96 h posttransfection (hpt) (Fig. 1B). The *vubi* knockout viruses, *vubi*KO and 2×KO-HA-*ac141*, had similar BV production but were equivalent to only 0.26% of WT levels. The *ac141* knockout viruses, *ac141*KO and 2×KO-Myc-*vubi*, had BV production reduced to only 0.005% of WT levels, which was similar to what has been previously described (11, 12). The double-knockout virus, *ac141*+*vubi*2×KO, and the control virus, *gp64*KO, did not produce any detectable BV. These results confirmed previous analyses showing that both AC141 and vUbi are required for BV production. In addition, the cumulative effect of knocking out both *vubi* and *ac141* results in the complete elimination of even the low level of virus observed with the single-gene KO viruses.

Coimmunoprecipitation of AC141 and vUbi. The elimination of BV production through simultaneous deletion of both *ac141*and *vubi* suggests these two proteins may interact. To study the possible association between AC141 and vUbi, coimmunoprecipitation experiments were performed. *Spodoptera frugiperda* IPLB-Sf21-AE clonal isolate 9 (Sf9) cells were infected with 2×KO-HA-*ac141*+Myc-*vubi* expressing N-terminal HA-tagged AC141 (HA-AC141) and N-terminally Myc-tagged vUbi (Myc-vUbi). As a control, Sf9 cells were infected with WT or *vubi*KO-Myc-vUbi, which expresses only Myc-vUbi and untagged AC141. Protein complexes were immunoprecipitated with anti-HA antibodies, and eluted material was analyzed by Western blotting. The input lanes showed that there was extensive ubiquitination of proteins with vUbi (Fig. 2A). HA-AC141 specifically coimmunoprecipitated Myc-vUbi-ubiquitinated proteins from 2×KO-HA-*ac141*+Myc-*vubi* virus-infected cells and not from the control samples (Fig. 2A). The Western blot identified two prominent proteins of approximately

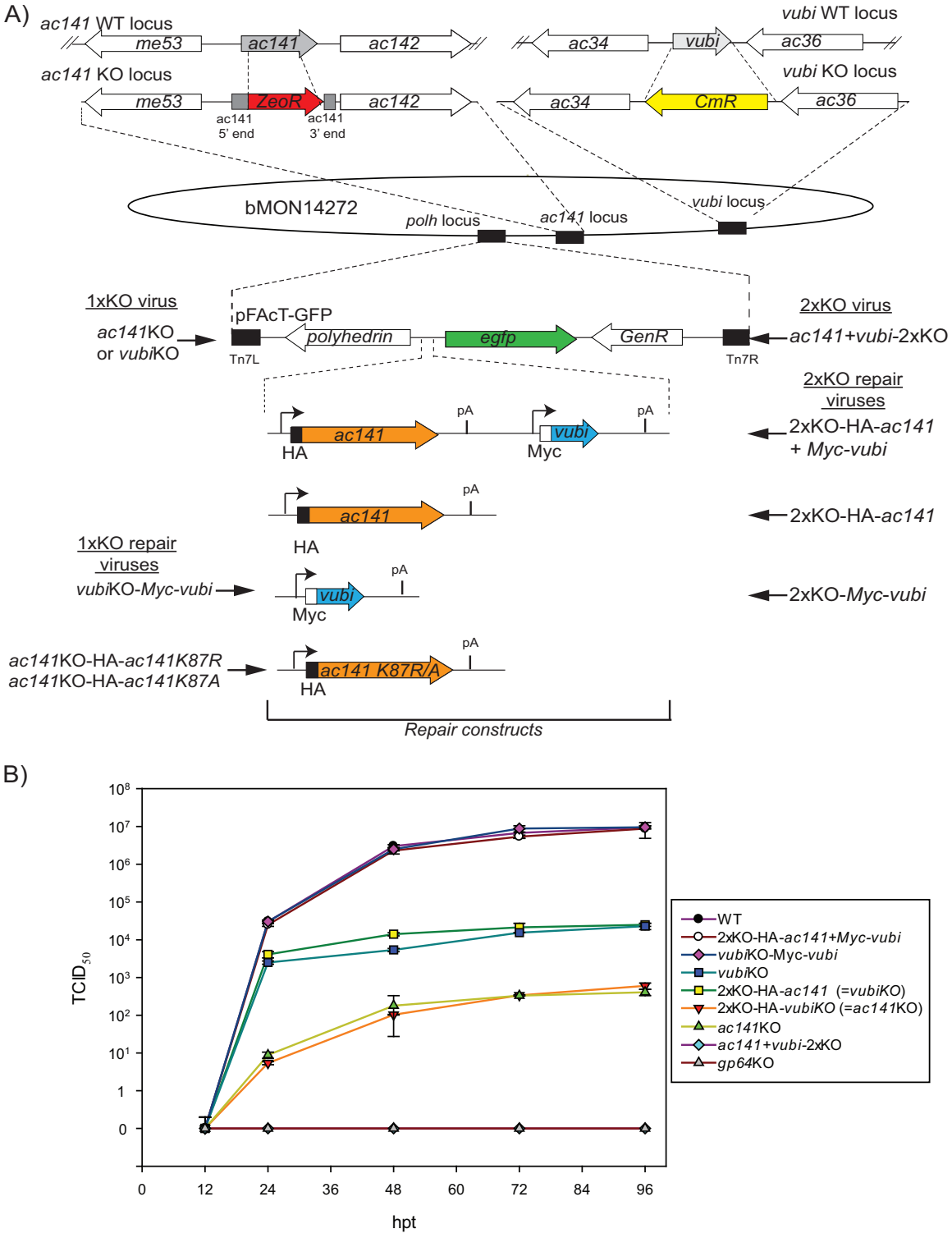

FIG 1 Construction of *ac141* and *vubi* single-knockout (1×KO) and double-knockout (2×KO) viruses and time course analysis of BV production. (A) Using the bacmid bMON14272, the *ac141*KO virus was generated by deleting the *ac141* ORF and replacing it with the zeocin resistance (ZeoR) gene. Similarly the *vubi*KO virus was generated by replacing the *vubi* ORF with the chloramphenicol resistance (CmR) gene. A double-knockout virus was generated by knocking out both *ac141* and *vubi* with zeocin and chloramphenicol resistance genes, respectively. The three KO viruses were repaired using pFAcT-GFP or pFAcT-GFP containing HA-*ac141*, Myc-*vubi*, or both genes. pFAcT-GFP contains the *egfp* marker gene, as well as *polyhedrin*. The resulting viruses were *ac141*+*vubi*2×KO, 2×KO-HA-*ac141*+Myc-*vubi*, 2×KO-HA-*ac141*, 2×KO-Myc-*vubi*, *ac141*KO, *vubi*KO, and *vubi*KO-Myc-*vubi*. The *ac141* KO virus was also repaired with two *ac141* mutants, *ac141K87R* and *ac141K87A*, generating the viruses *ac141*KO-HA-*ac141K87R* and *ac141*KO-HA-*ac141K87A*. (B) Analysis of BV production at 12, 24, 48, 72, and 96 hpt. Sf9 cells were transfected with 2 μg of bacmid DNA of each virus. The media containing the BV were collected at different time points and assayed for BV production by 50% endpoint dilution assay ($TCID_{50}$). Each data point represents a set of four biological repeats, and the error bars represent standard errors.

TABLE 1 Summary of viruses used in this study

Gene KO	Repair[a]	Virus name	Phenotype
ac141	*ph + gfp*[a]	*ac141*KO	*ac141* KO
vUbi	*ph + gfp*	*vubi*KO	*vubi* KO
vUbi	*Myc-vubi + ph + gfp*	*vubi*KO-*Myc-vubi*	WT
ac141 + vubi	*ph + gfp*	*ac141*+*vUbi*-2×KO	*ac141 + vUbi* KO
ac141 + vubi	*HA-ac141 + Myc-vUbi + ph + gfp*	2×KO-*HA-ac141*+*Myc-vUbi*	WT
ac141 + vubi	*HA-ac141 + ph + gfp*	2×KO-*HA-ac141*	*vubi* KO
ac141 + vubi	*Myc-vubi + ph + gfp*	2×KO-*vubi*KO	*ac141* KO
ac141	*HA-ac141K87R + ph + gfp*	*ac141*KO-*HA-ac141K87R*	*HA-ac141K87R*
ac141	*HA-ac141K87A + ph + gfp*	*ac141*KO-*HA-ac141K87A*	*HA-ac141K87A*
ac141	*HA-ac141 + ph + gfp*	*ac141*KO-*HA-ac141*	WT
ac66	*HA-ac66 + ph + gfp*	*ac66*KO-*HA-ac66*	WT
vp80	*HA-vp80 + ph + gfp*	*acvp801*KO-*HA-vp80*	WT
	ph + gfp	WT	WT

[a]*ph*, polyhedrin; *gfp*, green fluorescent protein.

37 and 45 kDa, along with other minor higher-molecular-mass proteins. These results showed that HA-AC141 associates either directly or in a complex with viral ubiquitinated proteins. Reciprocal coimmunoprecipitation was also done to confirm the association of AC141 and Myc-vUbi (Fig. 2B). As shown in Fig. 2B, the input lane showed numerous proteins that were ubiquitinated with Myc-vUbi. As expected, the majority of the viral ubiquitinated proteins were specifically pulled down with anti-Myc. The 26-kDa HA-AC141 was not detectable in the coimmunoprecipitations with Myc-vUbi. This suggests that only a small fraction of the extensive number of Myc-tagged viral ubiquitinated proteins interact with HA-AC141.

Mass spectrometric analysis of proteins coimmunoprecipitated with HA-AC141 to identify potential substrates and viral ubiquitination sites. Mass spectrometry (MS) analysis of the coimmunoprecipitated material with HA-AC141 was performed to identify the viral proteins that potentially interact with AC141 and are associated with BV development and egress. The MS analysis was applied to total pulldown eluent and material gel purified from the region containing the prominent Myc-Ubi-tagged 37- and 45-kDa proteins (Fig. 2A and Table 2). In addition to AC141, a number of the major BV structural proteins were detected, including VP80, VP39, GP41, P78/83, vUbi, GP64, and AC66. VP39 is the most abundant nucleocapsid protein. VP80 interacts with the F-actin cytoskeleton and is required for the movement of nucleocapsids from the nuclear virogenic stroma to the nuclear periphery regions (30). GP41 is a tegument protein required for nucleocapsid egress from the nucleus and efficient BV production (31, 32). P78/83 is required for actin nucleation during entry and is located at the base of the nucleocapsid (33, 34). GP64 is the major BV envelope protein, and AC66 is a nucleocapsid protein required for BV production, as deletion of *ac66* results in nucleocapsids that do not egress from the nucleus (35, 36). The primary proteins specific to the 35- to 45-kDa region (Table 2) were identified as ChiA, AC141, ODV-EC27, GP37, VLF-1, and AC114, but of these, only AC141 is essential for BV production.

MS analysis of AC141-coimmunprecipited proteins was also utilized to identify potential ubiquitination sites on the coimmunoprecipitated proteins. Ubiquitinated peptides increase in mass by the terminal GG from ubiquitin. The C terminus of vUbi, however, is GGY, but it is believed that any C-terminally modified ubiquitin-like molecules are trimmed by isopeptidases prior to any ubiquitin ligase event. It is known that cellular ubiquitins, even with one extra amino acid at the C terminus, are cleaved to make ubiquitin functional (37, 38). In case the vUbi C-terminal tyrosine was not cleaved, peptides were also analyzed for a GGY modification. Ubiquitinated peptides were detected only in the gel-purified 30- to 50-kDa region, and they were found to originate from AC141 at K87 (Fig. 2C and Table 2). Interestingly, two different mass-shifted peptides from the same AC141 sequence were identified, corresponding to a GGY and a GG modification at K87. The K87 ubiquitination site is located in the

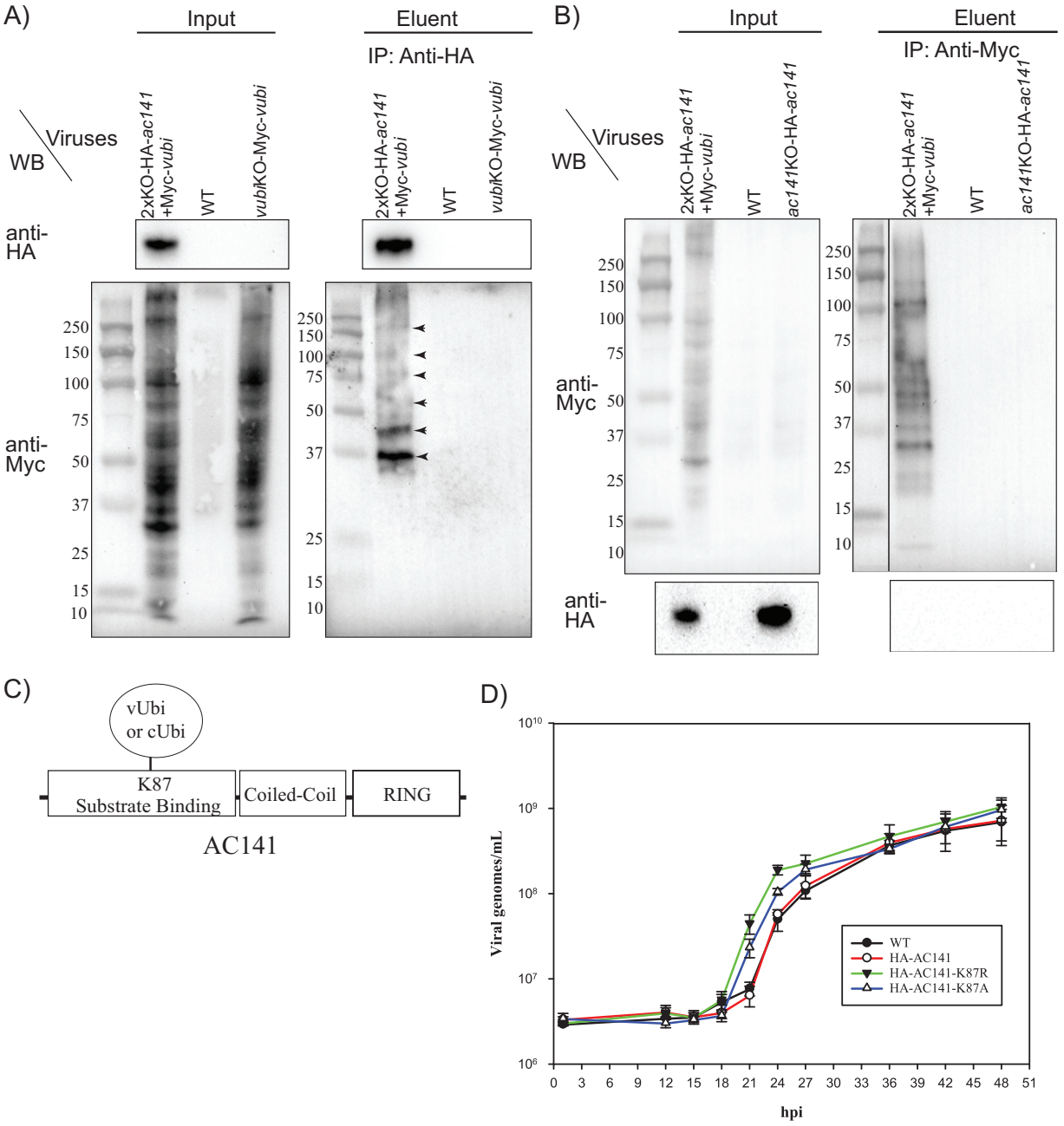

FIG 2 Coimmunoprecipitation of HA-AC141 and Myc-vUbi and impact of AC141 K87 mutations on BV production. (A) Sf9 cells were infected with 2×KO-HA-*ac141*+Myc-*vubi*, the WT, or *vubi*KO-Myc-*vubi*. Infected cells were harvested at 24 hpi, and total cell lysates were pulled down with HA beads and subjected to Western blot (WB) analysis. The input lanes were loaded with 0.25% of the total input, and the eluent lanes were loaded with 20% of the total eluent. The blots were probed with the antibodies indicated on the left. IP, immunoprecipitation. (B) Sf9 cells were infected with 2×KO-HA-*ac141*+Myc-*vubi*, the WT, and *ac141*KO-HA-*ac141*. The virus *ac141*KO-HA-*ac141* has been previously described (29). Infected cells were harvested, and total cell lysates were pulled down with anti-Myc antibody bound to protein G beads. The input lanes were loaded with 0.25% of the total input, and eluent lanes were loaded with 20% of the total eluent. The blots were probed with the antibodies indicated on the left. The marker lane was from the same gel and was moved to be adjacent to the sample lanes. The numbers on the left of the gels are kilodaltons. (C) Schematic diagram showing the RING, coiled-coil, and putative substrate binding domains of AC141. Also indicated is the location of the viral ubiquitination site of the substrate binding site of AC141 at lysine residue 87 (K87). (D) Sf9 cells were infected with the WT, HA-AC141, and mutant viruses *ac141*KO-HA-*ac141K87R* and *ac141*KO-HA-*ac141K87A* at an MOI of 5, and BV production was determined at 1, 12, 15, 18, 21, 24, 27, 36, 42, and 48 hpi. The media containing the extracellular virus or BV were collected at each time point, and the titer was determined by droplet digital PCR. Each data point shown represents a set of two biological repeats and two technical repeats. The error bars represent standard errors.

potential substrate binding region of AC141 (Fig. 2C). This result, therefore, suggests that vUbi might become attached to AC141 with a novel isopeptide linkage of tyrosine to lysine, as well as the normal glycine-lysine linkage. Overall, the MS results show that AC141 and vUbi interact during viral infection.

TABLE 2 Most prominent AcMNPV proteins known to be associated with BV or BV synthesis and transport, coimmunoprecipitated with HA-AC141 and identified by mass spectrometry

Protein source[a]	AcMNPV protein	ORF	No. of peptides		Sequence coverage (%)		Ubiquitin modification site (K) and type (GG or GGY)	Reference(s)
			HA-AC141 IP	Control	HA-AC141 IP	Control		
Total	VP80	*ac104*	11	0	20.3	0		30
Total	ChiA	*Ac126*	9	0	19.2	0		72
Total	VP39	*ac89*	8	0	28.8	0		73
Total	AC141	*ac141*	8	0	29.1	0		11, 12
Total	P40	*ac103*	6	0	14.7	0		72
Total	P49	*ac142*	6	0	14.9	0		74
Total	P78/83	*ac9*	5	0	11.8	0		33, 75
Total	39k/pp31	*ac36*	5	0	27.3	0		35
Total	IE1	*ac147*	5	0	13.9	0		76
Total	GP41	*ac80*	5	0	19.3	0		32
Total	FP	*ac61*	3	0	15	0		35
Total	PTP	*ac1*	3	0	19.6	0		35
Total	bro	*ac2*	3	0	11.2	0		77
Total	VLF-1	*ac77*	3	0	8.7	0		35
Total	vUbi	*ac35*	2	0	23.4	0		18
Total	GP64	*ac128*	2	0	5.1	0		28
Total	AC66	*ac66*	2	0	2.8	0		36
30–50	ChiA	*Ac126*	22	14	47.7	24.7		72
30–50	AC141	*ac141*	19	7	61.3	22.6	K87-GGY and K87-GG	11, 12
30–50	ODV-EC27	*ac144*	6	3	49.7	27.6		35
30–50	GP37	*ac64*	8	3	45	17.2		78
30–50	VLF-1	*ac77*	8	5	20.8	9.7		35
30–50	AC114	*ac114*	7	3	20.8	9.7		35

[a]Total, proteins identified from the total eluent of the AC141 immunoprecipitation (IP); 30–50, proteins isolated from the 30- to 50-kDa gel fragment of the AC141 pulldown eluent.

Mutational analysis of the AC141 K87 vUbi ubiquitination site to determine the effect on BV production. AC141 coimmunoprecipitated viral ubiquinated proteins, and in addition, using MS, it was found that AC141 was ubiquitinated at K87. Autoubiquitination of E3 ubiquitin ligases can act as a regulatory mechanism and can result in either enhancing substrate ubiquitination or signaling its own degradation (39–43). To investigate the significance of the AC141 ubiquitination, viruses were generated that mutated the K87 of HA-AC141 to arginine (K87R) or alanine (K87A) (Fig. 1A). A time course of virus production was performed and showed that mutation of AC141 K87 to arginine or alanine altered temporal aspects of BV production (Fig. 2D). In WT-infected cells, BV production initiates between 15 and 18 h postinfection (hpi) with an exponential increase between 21 and 27 hpi. In comparison, the K87R and K87A viruses both initiated BV production at the same time as the WT, with an exponential increase between 18 and 24 hpi, 3 h earlier than the WT. Compared to the WT, both mutant viruses produced nearly a log-unit-higher level of BV by 21 hpi, but maximum BV levels were similar at later times postinfection. These results indicated that the mutation of K87, to prevent AC141 ubiquitination at the site, results in more rapid production of BV.

Western blot analysis of purified BV and ODV for viral and cellular ubiquitinated proteins. If, as was hypothesized, vUbi is required to differentiate nucleocapsids destined for BV or ODV, possibly catalyzed by AC141, then the two forms of virions could potentially be differentially ubiquitinated. To address this, BV and ODV were purified from *vubi*KO-Myc-*vUbi*-infected Sf9 cells by sucrose density gradient and separated into envelope and nucleocapsid fractions. Total and fractionated protein samples were analyzed by Western blotting. The results showed that BVs contained approximately 4-fold-higher levels of vUbi than ODV (Fig. 3A). Fractionated samples showed that the vast majority of viral ubiquitinated proteins were in the nucleocapsid fraction. In addition, there was a specific viral ubiquitinated major band of approximately 100 kDa in the nucleocapsid fraction of BV, but not in the ODV (Fig. 3A, arrow). There were also other minor bands (indicated by asterisks), which were also present in ODV nucleocapsids, of approximately 86 kDa, 45 kDa, 43 kDa, 30 kDa, and 8 kDa

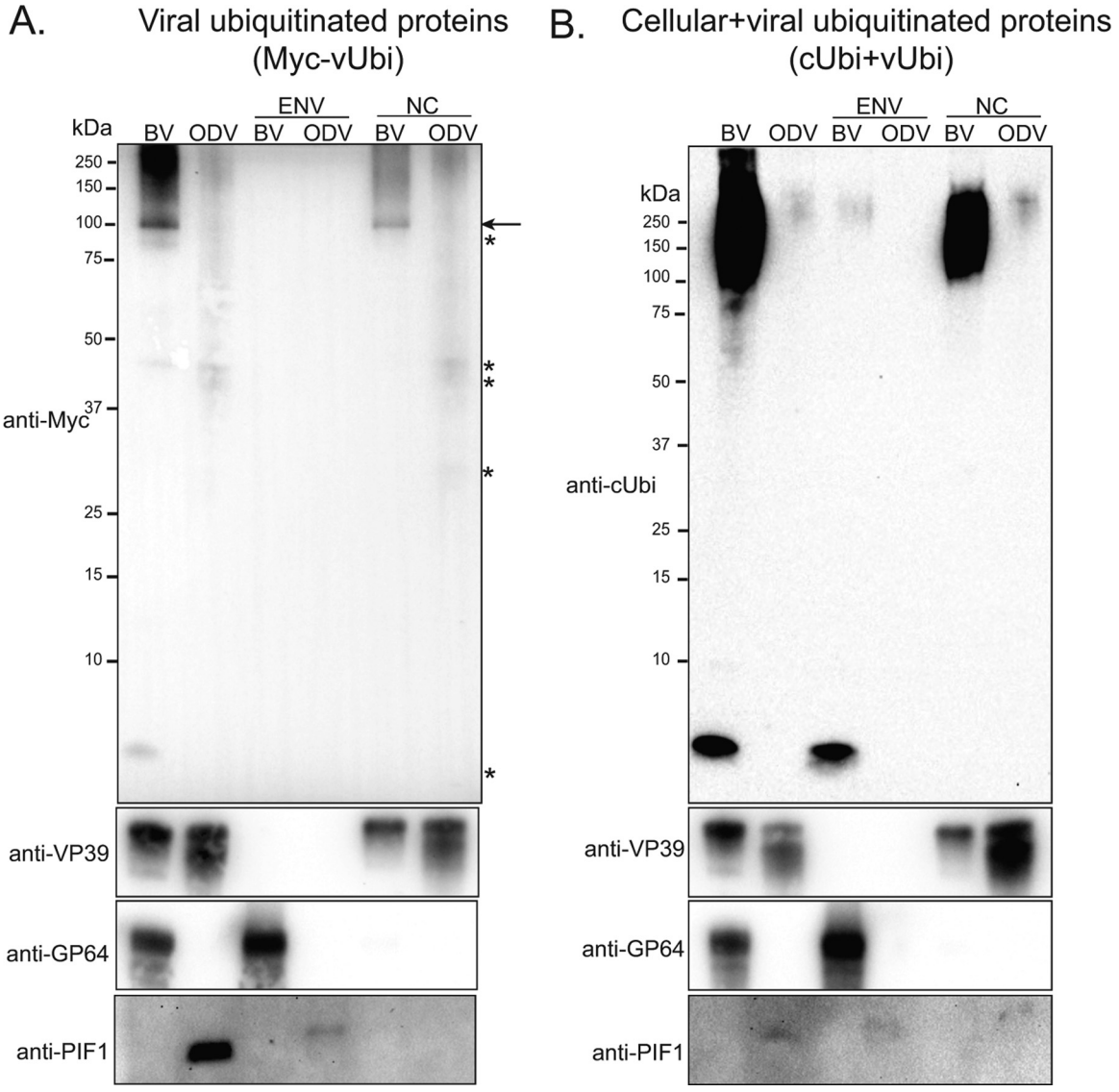

FIG 3 Western blot analyses of the isolated BV and ODV for viral ubiquitinated proteins. BV and ODV were purified from Sf9 cells that were infected with *vubi*KO-Myc-*vbi*. Purified BV and ODV were fractionated into envelope (ENV) and nucleocapsid (NC) fractions, separated by SDS-PAGE, and analyzed by Western blotting. The blots were probed with anti-Myc antibody to identify proteins ubiquitinated by vUbi (A) or with anti-cellular ubiquitin antibody to identify proteins ubiquitinated by cUbi and vUbi (B). Control blots using antibodies against the nucleocapsid protein VP39, the BV envelope protein GP64, and the ODV envelope protein PIF-1 to confirm the efficiency of fractionation are shown below. The arrow in panel A indicates a specific viral ubiquitinated major band of approximately 100 kDa in the nucleocapsid fraction of BV, but not in the ODV, while the asterisks mark other minor bands of approximately 86 kDa, 45 kDa, 43 kDa, 30 kDa, and 8 kDa that were also present in BV or ODV nucleocapsids upon long exposures.

(Fig. 3A). A very long exposure revealed that trace amounts of vUbi could also be detected in the envelope of BV, but not ODV. To examine total ubiquitination levels of both vUbi and cUbi in purified BV and ODV, a duplicate Western blot was performed and probed with anti-cUbi, which detects both cellular and viral ubiquitin (Fig. 3B). The results showed that BV was 80-fold more ubiquitinated than ODV. Most of the cellular and viral ubiquitin detected with anti-cUbi antibody is in the high-molecular-weight proteins of the nucleocapsid fractions of both BV and ODV. A low level of ubiquitin was also detected in the envelope fraction of BV, but not ODV. The higher levels of ubiquitin detected in the BV envelope with anti-cUbi antibody suggest it must be predominantly cellular in origin (Fig. 3A). To ensure correct fractionation of BV and ODV, blots were probed with antibodies to the nucleocapsid protein VP39, the BV envelope protein GP64, and the ODV envelope protein PIF-1 (Fig. 3A and B).

TABLE 3 Most prominent AcMNPV proteins in the region of 85 to 110 kDa of purified BV identified by mass spectrometry

AcMNPV protein	ORF	BV nucleocapsid or envelope protein	No. of peptides	Sequence coverage (%)	Mass (kDa)	Ubiquitin modification site (K) and type (GG or GGY)	Required for BV production (reference)
VP80	*ac104*	Nucleocapsid	33	50.8	79.9	None	Yes (30)
AC66	*ac66*	Nucleocapsid	29	38.2	94	None	Yes (36)
F protein	*ac23*	Envelope	25	39	79.9	K237-GG	No (65)
P94	*ac134*	Unknown	18	29	94.5	None	No (44)
GP64	*ac128*	Envelope	16	29.4	60.6	K232-GG and K299-GG	Yes (27, 28)
P78/83	*ac9*	Nucleocapsid	14	31.5	60.7	None	Yes (33, 79)
Helicase	*ac95*	Unknown	10	8.9	143	None	No (80)
LEF3	*ac67*	Unknown	9	29.6	44.6	None	No (81)

MS analysis of purified BV and ODV for potential viral ubiquitinated peptides. Western blot analyses showed that an approximately 100-kDa protein was specifically ubiquitinated in BV, but not in ODV. To identify the proteins in the 100-kDa band, the region from 85 to 110 kDa of an SDS-PAGE gel was isolated and analyzed by MS (Table 3). Similar to previously reported BV MS results (35), three known BV structural or associated proteins in the 100-kDa size range were identified: VP80 (80 kDa), AC66 (94 kDa), and F protein (80 kDa). F protein is an envelope protein, whereas AC66 and VP80 are both nucleocapsid proteins. It is therefore possible that either AC66 or VP80 is the viral ubiquitinated 100-kDa protein detected in BV (Fig. 3A). AC66 is required for nucleocapsid egress from the nucleus, and VP80 is required for movement of nucleocapsids from the virogenic stroma to nuclear periphery regions. These results suggested that AC66 or VP80 could be the potential substrate for viral ubiquitination in BV nucleocapsids. Both AC66 and VP80 were also identified as proteins that interact with AC141 (Table 2). P94 was also isolated from the 100-kDa region, but it is known not to impact BV development (44).

Coimmunoprecipitation analysis of Myc-vUbi with AC66 or VP80. If AC66 or VP80 is ubiquitinated by Myc-vUbi, then it should be possible to immunoprecipitate the 100-kDa viral ubiquitinated nucleocapsid protein with either VP80 or AC66. To enable this analysis, two viruses were constructed that expressed HA-tagged AC66 (*ac66*KO-*ac66*-HA) or VP80 (*vp80*KO-*vp80*-HA) (Fig. 4 and Table 1). Each virus (*ac66*KO-*ac66*-HA and *vp80*KO-*vp80*-HA) was coinfected with *vubi*KO-Myc-*vubi* or the WT (control virus with no epitope tag). At 24 hpi, cells were harvested, the supernatants were immunoprecipitated, and the eluents were analyzed by Western blotting. The Western blots showed the expression of VP80-HA-, AC66-HA-, and Myc-vUbi-tagged proteins in the input lanes (Fig. 5A). Coimmunoprecipitation of proteins from VP80-HA- and Myc-vUbi-expressing cells did not detect any vUbi-conjugated proteins in the eluent. In contrast, analysis of *ac66*KO-*ac66*-HA-infected cells showed that AC66-HA specifically coimmunoprecipitated a Myc-vUbi-conjugated protein of approximately 100 kDa (Fig. 5A). The coimmunoprecipitated band was of approximately the same size as the major vUbi-conjugated band from BV nucleocapsids (Fig. 3A). This result indicates that either AC66 is ubiquitinated by vUbi or it interacts with a 100-kDa vUbi-conjugated protein.

If AC66 is the target of vUbi ubiquitination, then HA-AC66-immunoreactive proteins should comigrate with the coimmunoprecipitated 100-kDa Myc-vUbi-conjugated protein. Therefore, a coinfection of *ac66*KO-*ac66*-HA and either *vubi*KO-Myc-*vubi* or WT was repeated and the cell lysates immunoprecipitated with anti-HA. Duplicate samples of the eluent material were separated on a 7.5% gel and probed with either anti-HA or anti-Myc to determine if the coimmunoprecipitated cellular AC66-HA and 100-kDa Myc-vUbi-conjugated protein comigrated (Fig. 5B). The Myc-vUbi band was observed to migrate approximately 7 to 10 kDa higher than the primary cellular AC66 band, which suggests that AC66 was monoubiquitinated. Longer exposures were used to determine if there were higher-molecular-mass species of AC66 that comigrated with the Myc-vUbi band; however, the signal from the primary HA-AC66 band occluded all higher-molecular-mass species (data not shown). This result suggested that if AC66 is ubiquitinated by vUbi,

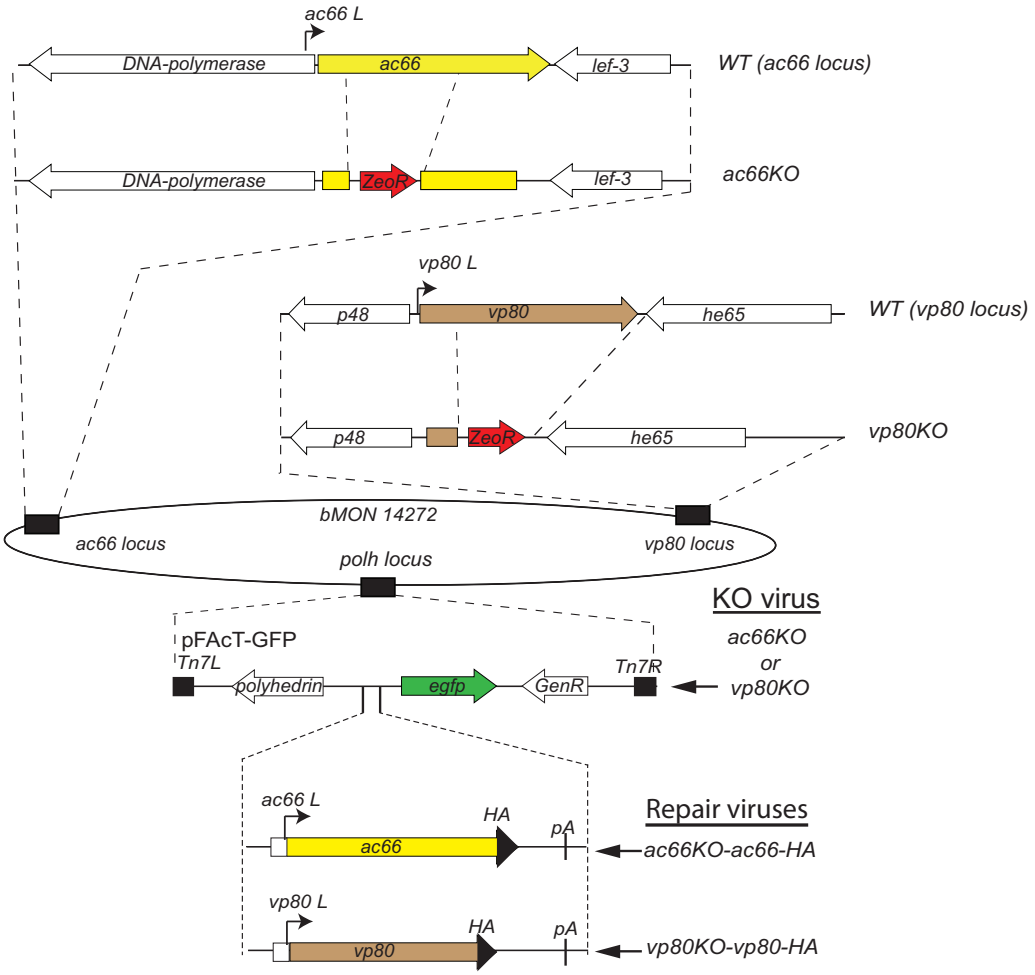

FIG 4 Construction of ac66 and vp80 KO and repaired bacmids. The schematic diagram shows how the *ac66*KO and *vp80*KO viruses were generated. The *ac66* or *vp80* ORF was deleted by recombination with the zeocin resistance gene. The *ac66*KO and *vp80*KO viruses were repaired using pFAcT-GFP containing either *ac66* or *vp80*, respectively, with a C-terminal HA tag. The viruses were named *ac66*KO-AC66-HA and *vp80*KO-VP80-HA.

it represents only a small proportion of the total cellular AC66. Therefore, to increase the proportion of any Myc-vUbi-conjugated AC66, we compared the Myc-vUbi and AC66-HA proteins in purified BV and ODV isolated from cells coinfected with *ac66*KO-*ac66*-HA and *vubi*KO-Myc-*vubi* (Fig. 5C). The purified BV and ODV samples were run side by side on a high-resolution SDS-7.5% PAGE gel, and duplicate lanes were probed with either anti-HA or anti-Myc. The Western blot showed that AC66-HA bands of higher molecular mass than its native size were present in the BV samples, but not in the ODV samples (Fig. 5C). The higher-molecular-mass HA-AC66 bands comigrated with the primary Myc-vUbi band that was present in BV but not ODV. This result supports the conclusion that AC66 is the target for vUbi ubiquitination, but only in BV nucleocapsids. MS analyses were performed on AC66-HA-coimmunoprecipitated material to identify potential AC66 ubiquitination sites. Two potential ubiquitination sites were identified on AC66, a high-probability site at K451 and a low-probability site at K91.

Coimmunoprecipitation of AC141 with AC66 or VP80. We further analyzed the interaction between AC66 and AC141 by coimmunoprecipitation and Western blotting. Sf9 cells were infected with *ac66*KO-*ac66*-HA or as controls with *vp80*KO-*vp80*-HA or the WT. The cell lysates were immunoprecipitated with anti-HA beads, and the eluents were analyzed by Western blotting and probed with a polyclonal antibody against AC141 or with anti-HA to detect AC66 or VP80. The input lanes showed expression of AC66-HA and VP80-HA, as expected (Fig. 6A). AC141 was expressed primarily as a 30-kDa protein,

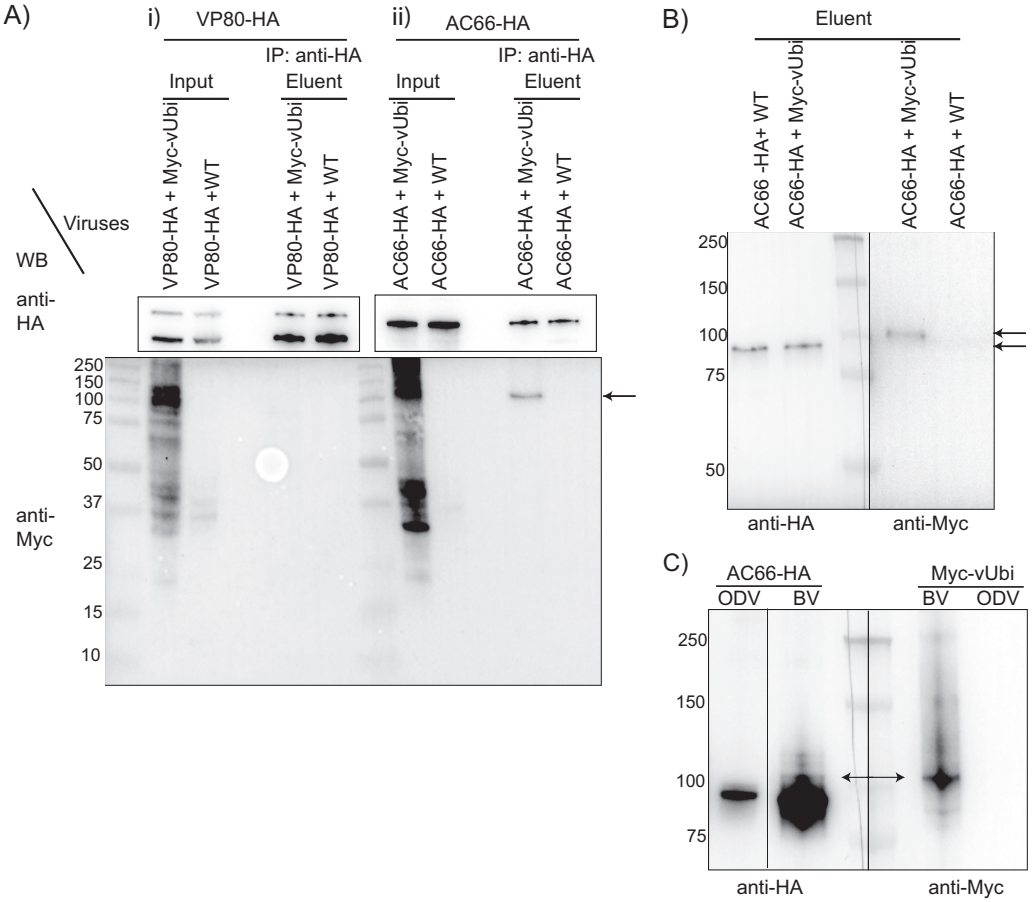

FIG 5 Coimmunoprecipitation analysis of AC66-HA or VP80-HA with Myc-vUbi. (A) Sf9 cells were coinfected with *vp80*KO-VP80-HA and *vubi*KO-Myc-vUbi or with *vp80*KO-VP80-HA and the WT (i) and with *ac66*KO-AC66-HA and *vubi*KO-Myc-vUbi or with *ac66*KO-AC66-HA and the WT (ii). Infected cells were harvested at 24 hpi, and total cell lysates were pulled down with HA beads. Samples were separated on SDS-12% PAGE gels and analyzed by Western blotting. The input lanes were loaded with 0.25% of the total protein, and the eluent lanes were loaded with 15% of the total eluent. The blots were probed with the corresponding antibodies listed on the left. The arrow on the right indicates the location of the Myc-vUbi immunoprecipitated by AC66. (B) The *ac66*KO-AC66-HA- and *vubi*KO-Myc-vUbi-infected cell eluent materials from panel A were separated in duplicate on an SDS-7.5% PAGE gel and blotted, and the two halves of the blot were probed with anti-HA (left) or anti-Myc (right) to determine if the detectable cellular forms of AC66 (94 kDa) comigrated with the 100-kDa viral ubiquitinated bands. The arrows indicate the positions of the dominant anti-HA- and anti-Myc-reactive bands. Each half of the blot represents different exposure times for each antibody, and the images were aligned using Adobe Photoshop. (C) BV and ODV were purified from Sf9 cells infected with *ac66*KO-AC66-HA and *vubi*KO-Myc-vUbi. Total virion protein was separated in an SDS-7.5% PAGE gel and analyzed by Western blotting. The membrane was cut in half at the ladder. The two halves of the blot were probed with anti-HA (left) or anti-Myc (right) to determine if the higher-molecular-mass forms of BV or ODV AC66 comigrated with the 100-kDa viral ubiquitinated bands. The double arrow shows the comigration of a 100-kDa AC66 band with the 100-kDa vUbi band. Each half of the blot probed with anti-HA and anti-Myc represents different exposure times; the images were aligned using Adobe Photoshop. The ODV and BV lanes of the anti-HA blot are from the same gel with the same exposure times, but intervening lanes were removed. The numbers on the left of the gels are kilodaltons.

along with two minor high-molecular-mass species. The eluent results showed that AC66-HA coimmunoprecipitated with the 30-kDa AC141. Surprisingly, however, a protein of approximately 80 to 90 kDa that was immunoreactive to the AC141 polyclonal antibody was also specifically coimmunoprecipitated. In contrast, no AC141 was coimmunoprecipitated with VP80-HA (Fig. 6A). Reciprocal coimmunoprecipitation was also done to confirm the association between AC66-HA and AC141. Sf9 cells were infected with *ac66*KO-*ac66*-HA and *vp80*KO-*vp80*-HA, and the cell lysates were pulled down with either AC141 polyclonal antibody or preimmune serum as the control. The input lanes showed the expression of AC141, AC66-HA, and VP80 in the corresponding lanes (Fig. 6B). AC66-HA, but not VP80-HA, was specifically coimmunoprecipitated by AC141. These results showed that AC66-HA interacts with AC141 during the course of

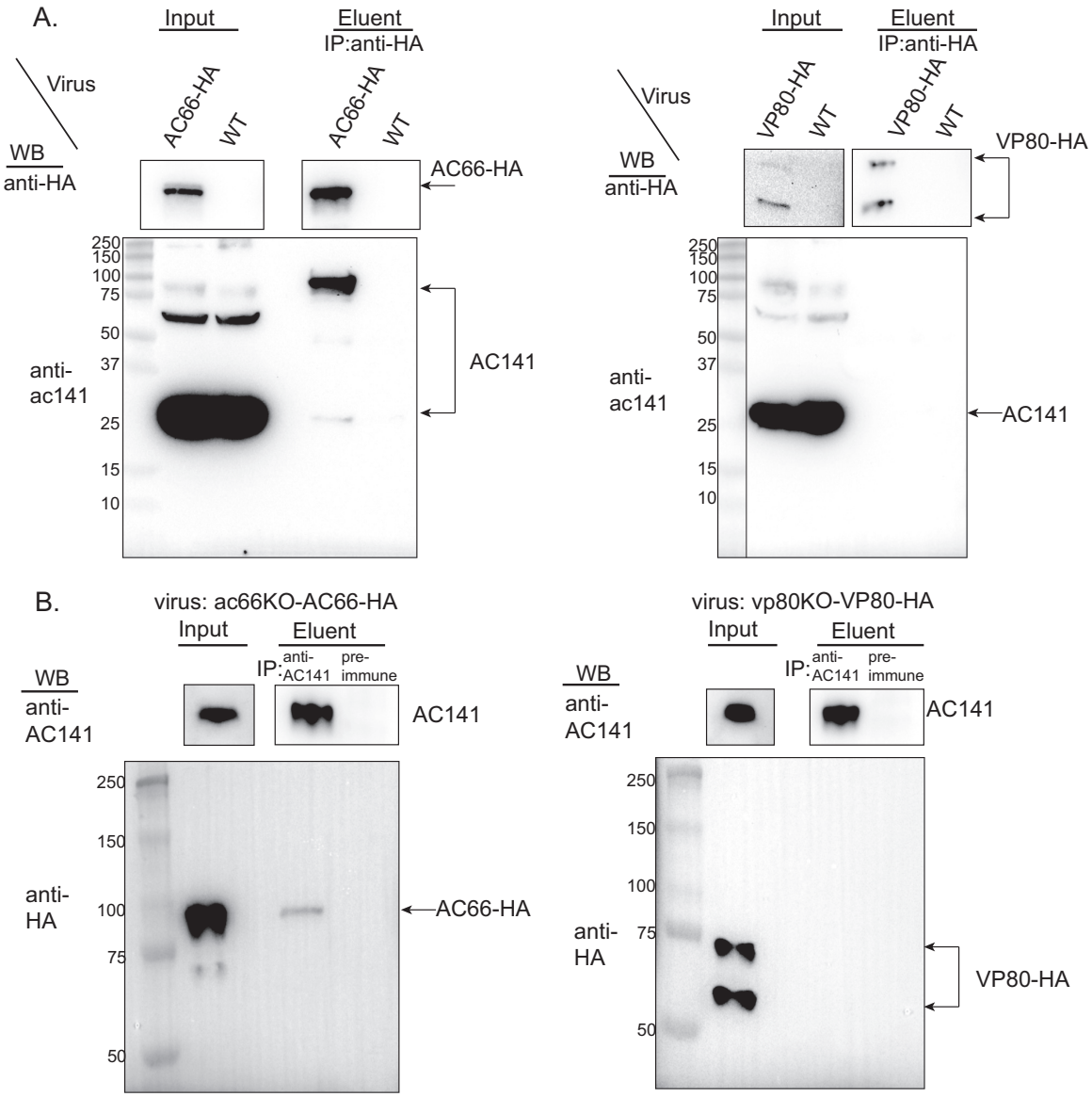

FIG 6 Coimmunoprecipitation analysis of AC66-HA or VP80-HA with AC141. To determine if AC141 interacts with either AC66 or VP80, Sf9 cells were infected with either *ac66*KO-AC66-HA, *vp80*KO-VP80-HA, or the WT as a control. Cell lysates from 24 hpi were immunoprecipitated (IP) with anti-HA (A) or anti-AC141 (B). The eluents were analyzed by Western blotting and probed with the respective antibodies indicated on the left of each blot. For the VP80 blot in panel A, the marker lane was from the same gel and was moved to be adjacent to the sample lanes. The numbers on the left of the gels are kilodaltons.

infection. The higher-molecular-mass form of AC141 that is specifically coimmunoprecipitated by AC66-HA could be polyubiquitinated or multiubiquitinated with 6 or 7 ubiquitin molecules. Neither the 30- or 90-kDa form of AC141 was coimmunoprecipitated by VP80-HA, which, like AC66, is a nucleocapsid protein. This specific interaction suggests that AC66 is a substrate for the predicted ubiquitin ligase activity of AC141.

Localization of AC66-HA and colocalization of AC66-HA with Myc-vUbi and AC141. The Western blot analysis, mass spectrometry, and coimmunoprecipitation data indicated that AC66 is specifically ubiquitinated in BV nucleocapsids by vUbi and suggests this process is mediated by AC141. To further analyze these interactions, confocal microscopy was performed to determine the cellular localization of AC66-HA and also to determine if AC66 colocalizes with Myc-vUbi and AC141. Sf9 cells were coinfected with *ac66*KO-*ac66*-HA and *vubi*KO-Myc-*vubi*, fixed at 24 hpi, and stained for AC66, vUbi, or AC141. As shown in Fig. 7A, AC66-HA was localized predominantly inside

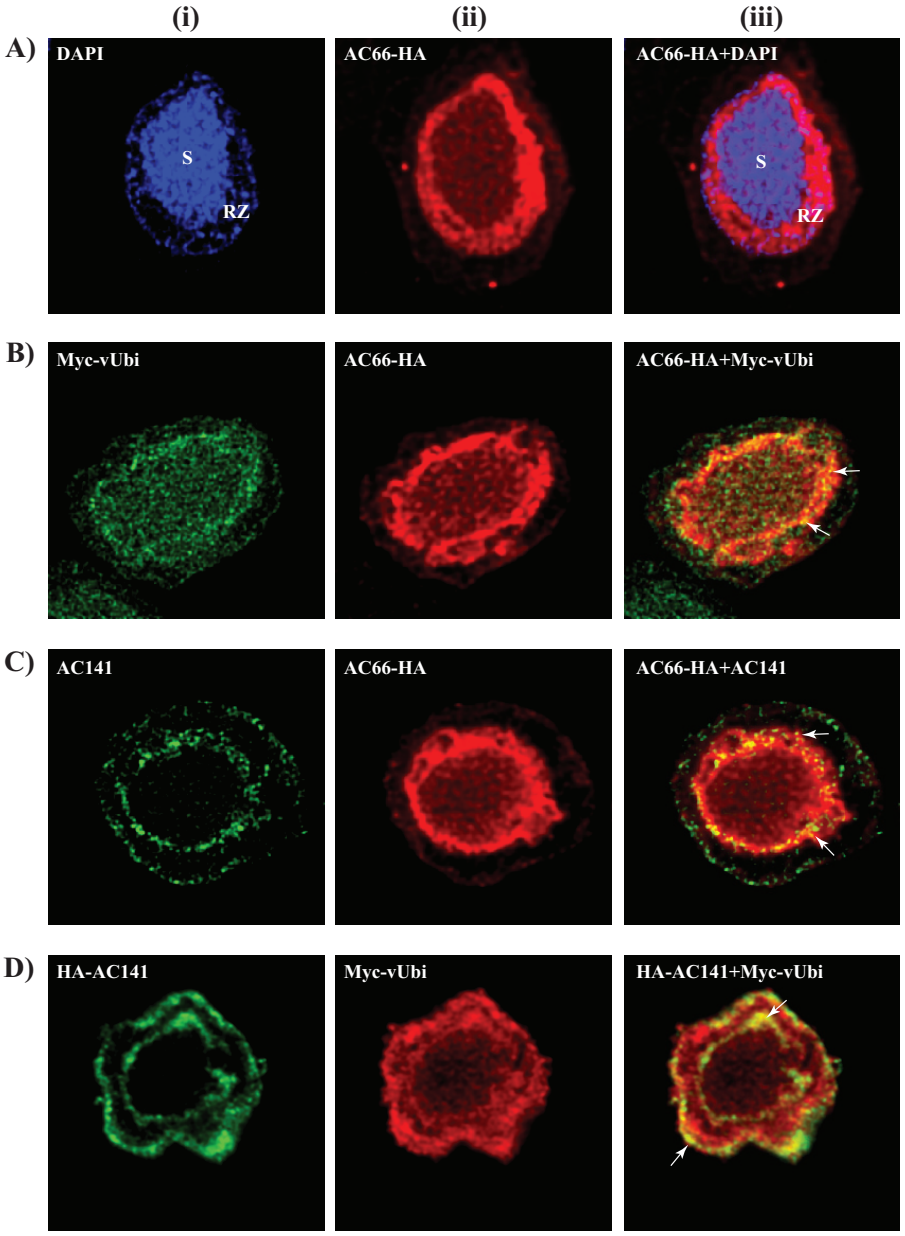

FIG 7 Colocalization analysis of AC66-HA, AC141, and Myc-vUbi. Sf9 cells were infected with *ac66*KO-AC66-HA (A), *ac66*KO-AC66-HA and *vubi*KO-Myc-vUbi (B), *ac66*KO-AC66-HA (C), or *ac141*KO-HA-AC141 and *vubi*KO-Myc-vUbi (D). The cells were fixed at 24 hpi and stained for AC66-HA (A), AC66-HA and Myc-vUbi (B), AC66-HA and AC141 (C), or HA-AC141 and Myc-vUbi (D) using anti-HA, anti-Myc, or anti-AC141 antibodies. The nuclear regions in panel A were stained with DAPI. Single staining (i and ii) and merged images (iii) are shown. Regions of colocalization are shown in yellow (arrows). S, virogenic stroma; RZ, ring zone.

the nucleus, with the majority of the signal in the ring zone, but lower levels were evenly distributed throughout the virogenic stroma. Small amounts of AC66 were also observed in the cytoplasm and at the plasma membrane. Myc-vUbi localizes throughout the cell in both the nucleus and cytoplasm (Fig. 7B and C). AC66-HA and Myc-vUbi exhibited colocalization that was primarily in the ring zone (Fig. 7B, iii). AC141 distribution was concentrated at both the nuclear and cytoplasmic peripheries, as shown previously (12). AC66-HA and AC141 showed colocalization, but only within the RING zone at the nuclear periphery in the regions outside the virogenic stroma (Fig. 7C, iii). Colocalization of HA-AC141 and Myc-vUbi was also analyzed in cells infected with

2×KO-HA-*ac141*+Myc-*vubi*. HA-AC141 and Myc-vUbi were observed to colocalize in both the nuclear and cytoplasmic periphery regions (Fig. 7D, iii). The colocalization analysis showed that the three proteins AC141, Myc-vUbi, and AC66-HA colocalize primarily in the ring zone of the nucleus outside the virogenic stroma. It is from this region that nucleocapsids either egress from the nucleus or are assembled into ODVs.

DISCUSSION

Baculoviruses are unique, as they produce two structurally different virions: BV, which is required for systemic transmission, and ODV, which is utilized for interhost transmission. Nucleocapsids for both virion types are synthesized in the infected cell nucleus in the virogenic stroma, from which they are transported to the nuclear periphery, called the ring zone. Nucleocapsids are either retained within the ring zone to form ODV or they egress from the nucleus, transit the cytoplasm, and bud from the plasma membrane to form BV. The focus of this study was to investigate the mechanism that determines how nucleocapsids are selected for nuclear egress and BV formation instead of remaining in the nucleus and forming ODV. AcMNPV encodes a predicted E3 RING domain ubiquitin ligase called AC141, as well as a viral ubiquitin that has 74% similarity to cellular ubiquitin. Both of these proteins had previously been shown to be specifically required for the production of BV. In this study, it was proposed that vUbi interacts with AC141 and that this interaction is required for the development of BV. The results have shown that AC141 and vUbi interact and that deletion of both the encoding genes eliminates BV production. In addition, nucleocapsids of BV, but not ODV, were shown to be extensively ubiquitinated by vUbi. Lastly, the nucleocapsid protein AC66 was identified as a potential substrate for AC141 and vUbi.

RING motifs of E3 ubiquitin ligases are required for binding E2 conjugating enzymes that are charged with ubiquitin (14). AC141 appears to be structurally distinct from the majority of E3 ubiquitin ligases, as it contains within the RING domain an extra cysteine residue adjacent to the third cysteine, and the histidine residue is replaced with tyrosine or phenylalanine (11). This suggests that AC141 may have a mechanistically different transfer of ubiquitin to a substrate. In cells infected with AcMNPV, there are both vUbi and cUbi in the cellular milieu. vUbi and cUbi are equally efficient in binding cellular E2s; however, vUbi is 40% less efficient than cUbi in transfer to a cellular E3 (21). This suggests a viral ubiquitin ligase is required for efficient recognition of the E2-vUbi complexes. The linkage of ubiquitin and E2 has been shown to be very flexible and to be able to exist in different structural orientations (45). However, upon binding of the E2-Ubi complex by the RING domain of an E3 ligase, the bound ubiquitin becomes locked into the active-site groove of E2 for catalysis (14). E3 ligases therefore have a close interaction with ubiquitin, and the structural differences of the AC141 RING motif may permit selective interaction with E2 enzymes conjugated with the structurally different vUbi as opposed to cUbi.

To study the interaction of AC141 and vUbi, single- and double-gene-knockout viruses were constructed and examined for their impacts on BV production. Deletion of *vubi* or *ac141* resulted in BV production being reduced to 0.26% or 0.005% that of the WT, respectively (Fig. 1B). When both *ac141* and *vubi* were deleted, BV production was eliminated, suggesting cooperative interaction between AC141 and vUbi. Deletion of *vubi* had a significant but smaller impact on BV production than deleting *ac141*. A possible reason for this is that, as described above, cUbi can be interchanged with vUbi in *in vitro* ubiquitination assays (21). It is therefore possible that in the absence of vUbi, cUbi may be utilized, albeit less efficiently, with a resulting decrease in BV production. E3 ubiquitin ligases are normally highly specific for their substrates (7), which suggests that deletion of *ac141* would result in the loss of substrate recognition and ubiquitination and therefore a more dramatic drop in BV production. The very low levels of BV that are observed in the *ac141* KO viruses (estimated to be $<$1.0 50% tissue culture infective dose [$TCID_{50}$] per 500 transfected cells) (Fig. 1B) could be explained by nonspecific stochastic tagging of nucleocapsids by cellular or viral E3 ligases from the pool of vUbi present in an infected cell. Deletion of both *ac141* and *vubi* would result

in neither of the potential compensation mechanisms being available, and therefore, no BV would be produced, which is what was observed (Fig. 1).

AC141 was also found to be a substrate for ubiquitination, as either viral or cellular ubiquitin was found to be linked to residues in the AC141 substrate binding domain. Autoubiquitination has been shown to downregulate E3 ubiquitin ligases by polyubiquitination and proteasome degradation or to upregulate them by monoubiquitination, resulting in the enhanced ubiquitination of target substrates (39–43). Mutation of the AC141 ubiquitination sites results in accelerated BV production, suggesting ubiquitination of AC141 may act as a switch mechanism to regulate its activity, which results in altered rates of BV production.

The C-terminal amino acids of cellular ubiquitins are normally diglycines, whereas vUbi has diglycine followed by a tyrosine. Inactive variants of cellular ubiquitin that have extra amino acids after the C-terminal diglycine exist, but they are normally cleaved by cellular isopeptidases or deubiquitinases (DUBs), resulting in functional ubiquitin (37, 38). Most ubiquitin binding proteins, including DUBs, bind cUbi at a hydrophobic surface or patch centered on I44 of cUbi (46). The vUbi I44 patch is conserved (38, 46); however, DUB binding domains have greater affinity for polyubiquitin or ubiquitin linked to a substrate than for free ubiquitin (47). AcMNPV vUbi is encoded as a monomer, whereas cUbi is usually expressed as a linear fusion of multiple ubiquitin molecules or with ribosomal proteins (37). As yet, no viral or cellular protein has been identified that has DUB activity and that can process vUbi to a diglycine C terminus. The C-terminal tyrosine of vUbi may play an important regulatory role, but this remains to be determined.

The envelope fraction from purified BV contained mainly monomeric cUbi and high-molecular-mass cUbi conjugates but also contained traces of vUbi (Fig. 3). Previous biochemical analyses of BV envelopes by Guarino et al. (20) showed that they contained two forms of monomeric ubiquitin, nonmodified or covalently linked to envelope phospholipid, in the proportions 80% cUbi and 20% vUbi. Similarly, this study also showed that in BV envelopes, cUbi makes up the majority of monomeric and conjugated ubiquitin. In other viral systems, cUbi has been shown to become associated with viral envelopes via the host endosomal sorting complex required for transport (ESCRT) pathway (10, 48). Viruses either encode E3 ubiquitin ligases or encode adapter proteins that recruit other components of ESCRT to support the process of budding from the plasma membrane. Interestingly, it has recently been shown that during baculovirus infection, ESCRT pathway components are required for BV production (49). If AcMNPV utilizes the host ESCRT components similarly to other viral systems, this could account for the specific cUbi and vUbi incorporation into the envelope or as conjugates attached to BV envelope proteins or lipids.

This study proposed that AcMNPV may utilize AC141 as a virus-specific E3 ubiquitin ligase to ubiquitinate nucleocapsids with vUbi to differentiate those that become BV or ODV. In support of this, a protein of approximately 100 kDa was found to be specifically ubiquitinated in the BV nucleocapsids but not in the ODV nucleocapsids (Fig. 3). Two of the potential nucleocapsid proteins in that region are AC66 and VP80 (30, 36). MS and coimmunoprecipitation analyses showed that AC141 associates specifically with AC66, which has also been shown to be required for nucleocapsid egress. Ke et al. (36) performed a detailed analysis of AC66 and proposed that AC66 and AC141 interact inside the nucleus to facilitate nucleocapsid egress. Two AC66 peptides were found by MS analysis to be modified by viral or cellular ubiquitin. Higher-molecular-mass forms of AC66 were identified in nucleocapsids, the dominant form of which was 7 to 10 kDa larger than its native size and comigrated with the nucleocapsid-specific 100-kDa viral ubiquitinated protein. The higher-molecular-mass form of AC66 is significantly enriched in BV compared to infected cells, where the vast majority of the AC66 exists in its native form and higher-molecular-mass species could not be resolved in total cell extracts. This was expected, because only approximately 2.3% of the viral genomes synthesized are utilized to form BV and the remaining 97.7% is retained inside the nucleus to form

the ODV (50). Overall, these results suggest that only a minor fraction of the total AC66 produced becomes ubiquitinated and that it is associated only with BV nucleocapsids.

Other viral systems use ubiquitination as a signal for the trafficking of nucleocapsids. For example, ubiquitination of the herpesvirus tegument protein pUL36 can act as a switch that determines capsid retrograde or anterograde cytoplasmic movement along microtubules, which can significantly impact neurovirulence (51–53). Nuclear egress of herpes simplex virus 1 (HSV-1) capsids has been extensively studied, and it is known that nucleocapsids egress from the nuclear envelope by utilizing a budding process. Several HSV-1-encoded proteins, including the pUL31-pUL34 nuclear egress complex, are associated with the inner and outer nuclear envelope membranes. These proteins assist in the budding of nucleocapsids from the nucleus and mediate the primary envelopment into the perinuclear space and de-envelopment from the outer nuclear envelope (54, 55). Recently, it was also shown that ubiquitination of the pUL34 homolog of Epstein-Barr virus (BFRF1) regulates the modulation of the nuclear envelope and nuclear egress of viral nucleocapsids (56). Although electron micrographs of AcMNPV-infected cells have suggested that nucleocapsids may also egress from the nucleus by budding through the nuclear envelope, definitive evidence is lacking (12, 57). Our coimmunoprecipitation and MS analyses suggested that, in addition to AC66, AC141 also interacts with GP41, which is known to be required for nuclear egress (32, 35). Interestingly, GP41 was found to associate with the SNARE (soluble *N*-ethylmaleimide-sensitive factor attachment protein receptor) proteins, which are required for fusion of transport vesicles with target membranes and for nuclear egress of AcMNPV nucleocapsids (58). It is possible that during egress of nucleocapsids from the nucleus, AC141, AC66, and GP41 form part of a nuclear-egress complex. The ubiquitination of nucleocapsid proteins, such as AC66, may therefore be part of the signaling process required for the recognition of nucleocapsids by a nuclear envelope complex composed of viral and cellular proteins. In support of this, confocal microscopy showed that AC141, AC66, and vUbi associate near the nuclear periphery regions (Fig. 7). AC66 may also play a role once nucleocapsids traverse the nuclear envelope, since the N terminus has a conserved desmoplankin domain. Desmoplankin domains can bind intermediate filaments and interact with microtubule components, which are known to be required for nucleocapsid egress (59–61). It is therefore possible that AC66 enables interaction with the cellular cytoskeleton during egress from the nucleus.

In summary, we have shown that the nucleocapsids that egress from the nucleus to form BV are differentially modified by extensive ubiquitination with vUbi compared to those used to form ODV. In addition, these data support the conclusion that AcMNPV AC141 is involved in the ubiquitination of the nucleocapsid protein AC66, or associated proteins, with vUbi to enable BV production. Ubiquitination with vUbi is therefore the potential mechanism by which a nucleocapsid is directed to become a BV, a critical event in the baculovirus replication cycle that enables systemic virus spread in an infected host.

MATERIALS AND METHODS

Cell lines and viruses. Sf9 cells were maintained in Grace's insect medium supplemented with L-glutamine, 3.33 g/liter lactalbumin hydrolysate, and 3.33 g/liter yeastolate (Gibco Life Technologies) and further supplemented with 10% fetal bovine serum at 27°C. The WT virus was AcMNPV-E2, and the AcMNPV-E2 bacmid used for construction of recombinant viruses was bMON14272 (62).

Construction of *vubi* knockout, *ac141* plus *vubi* double-knockout, and repaired viruses. The *vubi* open reading frame (ORF) is close to *ac34*, and the late promoter sequence of *ac34* is within the *vubi* ORF (63). Upon deletion of *vubi*, the late promoter sequence for *ac34* was reintroduced in the primers used to amplify the chloramphenicol resistance gene. The primer sequence to amplify the *cat* gene was based on previously published sequences (64, 65). The *cat* gene was PCR amplified using the plasmid pKD3 as the template with primer pair 746-747 (Table 4; the core late promoter sequence for *ac34* in the 746 primer sequence is underlined). The PCR product was gel purified and transformed into bMON14272 containing *Escherichia coli* BW25113/pKD46 electrocompetent cells (64). The recombinant cells were selected, and correct insertion of the *cat* gene in the *vubi* locus was confirmed with primer pairs 763-764 and 765-766 (Table 4), which confirmed recombination into the correct locus.

The *ac141* and *vubi* double-knockout AcMNPV bacmid was generated by using a strategy similar to that described above (64). The *ac141* ORF was knocked out using a 2.9-kbp EcoRI-HindIII restriction

TABLE 4 Primers used for construction of plasmid clones and viruses

Primer no.	Primer sequence (5′ to 3′)
2587	GCTTTTTTTATTACTATGATCAAT
2588	GATTCTCTATTCTATGCTTGTACA
2589	CCTTTTTTTATTACTATGATCAAT
2590	CATTCTCTATTCTATGCTTGTACA
746[a]	CAAGGGCGCATTCACAGCAACCGTTGTCATTTATAAGTAAACTTATCTAAGTGTAGGCTGGAGCTGCTTC
747	CAAGATACAAATATGTCAGATTAAATAAAAAACTTTTATGTATATTTAATGATATGAATATCCTCCTTAG
763	TGTGAATAAAGGCCGGATAAAACT
764	CCCATTAGCGGCAGCAGGAAA
765	GTCGGCGTGCGTGTAACAAAGT
766	CAAGGCGACAAGGTGCTGATGC
1833	ACACCGGTAAAATGCAAGAACAAAAACTTATTTCTGAAGAAGATCTTATATTCATCAAAACAT
1834	GG TCTAGAAATAAAAAACTTTTATGTATATTTA
1835	CCCTGCAGATCAATTGTG
1313	GCAACTGTGACGCCATAG
1239	CTGACCGACGCCGACCAA
1629	GCGTCTAGATGCTTTGTTTCTTTCGTATT
1630	GCGGCGGCCGCTTAGGCGTAGTCGGGCACGTCGTAGGGGTATTCGACGTTTGGTTGAAC
1695	GCGCTGCAGGTACCTGTTTGATAAACTC
1696	GCGTCTAGATTAGGCGTAGTCGGGCACGTCGTAGGGGTATATAACATTGTAGTTTGCGTT
1266	CGGATTTCGCCGGCCGAGATATCAACACGTTGACGCACAACATCAACTACTTCGGATCTCTGCAGCAC3
1267	TTGTCGCGACTTGAGACAATTCATTTTTAGTTGCAGTTAATTCATTTACATCGAGGTCGACCCCCCTG
1268	CGCGCACTGTACACGATT
1014	CCGATATACTATGCCGATGATT
1310	GAAGAGTGTTATGTTAAAATTGATAGACTATTTAAAGAGAGCATTAAAAATTCGGATCTCTGCAGCAC
1311	TTATATAACATTGTAGTTTGCGTTCATCAACATTATTAGTCTTTGCAAATTCGAGGTCGACCCCCCTG
1312	GCCGCGGGTAACAT

[a]The underlined region in the 746 primer sequence is the core late promoter sequence for *ac34*.

fragment from the previously described plasmid vector pAc-exon0-KO (11). The restriction fragment contained the 483-bp zeocin resistance gene under the control of the EM7 promoter and 1,547 bp of 5′ and 543 bp of 3′ *ac141* flanking sequences. The 5′ flanking sequence contained 142 bp of the 5′ ORF of *ac141*, which contains the splice site of *ie0* and the 3′ flanking sequence of the promoter downstream of *ac142* (11). The restriction fragment was transformed into *E. coli* BW25113/pKD46 competent cells containing the *vubi*KO bacmid. The recombinant cells were selected, and correct insertion of the zeocin resistance gene in the *ac141* locus was confirmed with primer pairs, as previously described (11). The double-gene-knockout bacmid containing the desired recombination was selected, and the resulting virus was named *ac141*+*vubi*2×KO.

The transfer vector pFAcT-GFP, which contains polyhedrin and enhanced green fluorescent protein (GFP) was used to repair the *ac141*, *vubi*, and *ac141*+*vubi* knockout bacmids. These plasmids were pFAcT-GFP-Myc-*vubi*, pFAcT-GFP-HA-*ac141*, and pFAcT-GFP-HA-*ac141*+Myc-*vubi*. To construct pFAcT-GFP-Myc-*vubi*, the *vubi* sequence was amplified with the primer pair 1833-1834 containing AgeI and XbaI sites. The primers also inserted the Myc epitope tag (EQKLISEEDL) coding sequence after the second codon of *vubi* (66) and the *vubi* poly(A) signal at the 3′ end.

The amplified 320-bp fragment was digested with AgeI and XbaI and ligated to a similarly digested vector that contained the *ac141* late promoter. The resulting plasmid, pMyc-*vubi*, was digested with XhoI and XbaI, which generated a 395-bp fragment [*ac141* late promoter plus Myc-*vubi* plus *vubi* poly(A)] that was inserted into pFact-GFP-digested with XhoI and XbaI, to generate pFAcT-GFP-Myc-*vubi*. The pFAcT-GFP-HA-*ac141* plasmid has been previously described (11). The pFAcT-GFP-HA-*ac141*+Myc-*vubi* plasmid was constructed as follows. Myc-*vubi*, along with the *ac141*promoter and the *vubi* poly(A) signal, was amplified by PCR, using pFAcT-GFP-Myc-*vubi* as a template, with the primer pair 1834 and 1835, which contained PstI and XhoI sites. The fragment was digested with PstI and XbaI and cloned into pFAcT-GFP-HA-*ac141* to generate the plasmid pFAcT-GFP-HA-*ac141*+Myc-*vubi*. The plasmids pFAcT-GFP, pFAcT-GFP-Myc-*vubi*, and pFAcT-GFP-HA-*ac141* or the pFAcT-GFP-HA-*ac141*+Myc-*vubi* bacmid was used to transform *E. coli* DH10B cells containing one of the knockout bacmids and the helper plasmid (pMON7124), which encodes the Tn*7* transposase, as described previously (62). The genotype was verified by PCR. Seven repaired bacmids were generated, which were called *ac141*KO, *vubi*KO, *ac141*+*vub*2×KO, *vubi*KO-*Myc*-*vubi*, 2×KO-HA-*ac141*+Myc, 2×KO-HA-*ac141*, and 2×KO-Myc-*vubi*.

Construction of *ac66* knockout, *vp80* knockout, and repaired viruses. *ac66* was deleted from the AcMNPV bacmid bMON14272, using recombination in *E. coli* as described above. The 5′ terminus of the *ac66* ORF contains the late promoter sequence of the adjacent *dnapol*, and the 3′ terminus contains the poly(A) region of the adjacent *lef3*. Therefore, 270 bp of the *ac66* 5′ terminus and 880 bp of the 3′ terminus were retained. The zeocin resistance gene was PCR amplified from p2ZeoKS with the primer pair 1266 and 1267 (Table 4), which also contain *ac66* homologous sequences. The PCR-amplified 625-bp fragment contains a zeocin resistance gene under the *EM7* promoter and the *ac66* flanking sequence for recombination. The amplified PCR product was transformed into electrocompetent *E. coli* BW25113/pKD46, and recombinants were selected as described above. The correct *ac66* deletion and insertion of

the zeocin resistance gene were confirmed by PCR with the primer pair 1268 and 1014 (Table 4). The deletion bacmid was named *ac66*KO.

The *vp80* ORF was deleted using the same method. Due to regulatory sequences of upstream genes, 473 bp in the 5′ terminus of the *vp80* ORF was retained, but the remaining ORF sequences were deleted. The zeocin resistance gene was PCR amplified from p2ZeoKS with primer pair 1310 and 1311, which also contain the *vp80* homologous sequences for recombination. Correct insertion of the zeocin resistance gene was confirmed with primer pairs 1312 and 1014, and also 1313 and 1239 (Table 4). The deletion bacmid was named *vp80*KO.

To generate a C-terminal HA epitope-tagged clone of *ac66*, the *ac66* late promoter and ORF were PCR amplified from the AcMNPV genome with primer pair 1629 and 1630, which contained a 5′ XbaI and a 3′ NotI site. The HA epitope nucleotide sequence was contained in the 3′ primer 1630 (Table 4). The PCR product was digested with XbaI and NotI and inserted into pFAcT-GFP-Tnie1PA digested with the same restriction enzymes, resulting in the clone pFAcT-GFP-AC66-HA. The *ac66*KO bacmid was repaired with pFAcT-GFP-AC66-HA using Tn*7*-mediated transposition, as described above, to generate the *ac66*KO-*ac66*-HA repaired virus. Similarly, the *vp80* late promoter and ORF, with a C-terminal HA epitope tag, were PCR amplified from the AcMNPV genome with the primer pair 1695 and 1696, which contain PstI and XbaI sites, respectively. The HA epitope nucleotide sequence was contained within the 3′ primer 1696. The PCR product was digested with PstI and XbaI and inserted into pFAcT-GFP-Tnie1PA digested with the same restriction enzymes. The resulting clone was named pFAcT-GFP-VP80-HA. The *vp80*KO bacmid was repaired with pFAcT-GFP-VP80-HA by Tn*7*-mediated transposition to generate the *vp80*KO-*vp80*-HA repaired virus.

Mutation in the ubiquitination site of AC141 (K87). The potential ubiquitinated lysine 87 of AC141 was mutated to an arginine or an alanine by inverse PCR. The PCR template was a previously constructed plasmid, p2Zeo-HA-Acexon0. Site-directed mutagenesis was carried out by standard PCR procedures using the primer pair 2587 and 2588 for K87R (AAA→CGC) and primer pair 2589 and 2590 for K87A (AAA→GCC). A 1.4-kbp XhoI and XbaI fragment excised from mutagenized p2Zeo-HA-Acexon0 was cloned into XhoI- and XbaI-digested pFAcT-GFP to produce pFAcT-HA-*ac141*-K87R and pFAcT-HA-*ac141*-K87A. These clones were used to repair the bacmid *ac141*KO, using the method described above, to generate the viruses *ac141KO-HA-ac141*-K87R and *ac141KO-HA-ac141*-K87A.

Time course analysis of virus infection in bacmid-transfected or virus-infected cells for analysis of BV production and viral protein synthesis. Sf9 cells were seeded into 6-well plates (2.0×10^6 cells per 35-mm-diameter well) and transfected with 1.0 μg of each bacmid or infected with BV at a multiplicity of infection (MOI) of 5 or 10. To measure BV production, the culture medium was harvested at various times posttransfection and centrifuged at 3,000 $\times$ *g* for 5 min to pellet cell debris. BV production was determined by the $TCID_{50}$ endpoint dilution assay or by droplet digital PCR (12, 67).

Coimmunoprecipitation of protein complexes. Sf9 cells (5.0×10^7) were infected with the respective viruses at an MOI of 10. Infected cells were harvested at 24 hpi and resuspended in 1.25 to 1.5 ml of either HEPES lysis buffer (15 mM HEPES, pH 7.6, 10 mM KCl, 0.1 mM EDTA, 0.5 mM EGTA, 1 mM dithiothreitol [DTT], and 1% protease inhibitor cocktail [Invitrogen]) or EBC lysis buffer (50 mM Tris-HCl, pH 8.0, 120 mM NaCl, 0.5% Nonidet P-40, 0.2 mM sodium orthovanadate, 1% sodium fluoride, and 1% protease inhibitor cocktail). Following cell lysis, the immunoprecipitation protocol was followed, as previously described (61). The eluent volume was vacuum concentrated to 60 μl and mixed with 20 μl of 4$\times$ protein sample buffer (PSB) (277.8 mM Tris-HCl, pH 6.8, 44.4% [vol/vol] glycerol, 0.02% bromophenol blue, 4% β-mercaptoethanol, 1% protease inhibitor cocktail [Sigma-Aldrich]). The sample was boiled for 10 min, subjected to SDS-polyacrylamide gel electrophoresis (PAGE) using Mini-Protean TGX stain-free gels (Bio-Rad), and examined by Western blotting.

Confocal microscopy. Sf9 cells were plated on sterile coverslips and allowed to settle overnight as previously described (61). The cells were infected with viruses at an MOI of 10. At different times postinfection, cells were fixed (100 mM HEPES, 5 mM $MgCl_2$, 5 mM EGTA, pH 6.9, and 1.5 or 4% formaldehyde) for 45 min, followed by permeabilization with 0.01% Triton X-100 solution in 1$\times$ PBS for 15 min. Incubation of primary and secondary antibodies was as previously described (61). The coverslips were mounted with Prolong Gold antifade reagent (Molecular Probes) with or without DAPI (4′,6′-diamidino-2-phenylindole). The primary antibodies included mouse monoclonal anti-c-Myc 9E10 (1:50; Santa Cruz Biotechnology), rabbit polyclonal anti-HA (1:200; Abcam), and rabbit polyclonal AC141 (1:400). The secondary antibodies used were goat anti-mouse Alexa-647 (1:500; Molecular Probes), goat anti rabbit Alexa-488 (1:500; Molecular Probes), goat anti rabbit Alexa-647 (1:500; Molecular Probes), goat anti mouse Alexa-405 (1:500; Molecular Probes), and goat anti rabbit Alexa-405 (1:500; Molecular Probes). All images were acquired using a Leica TCS SP8 confocal laser scanning microscope (CLSM) with a 63$\times$ oil immersion lens. Samples were sequentially excited at 488 nm for Alexa-488 or GFP, 633 nm for Alexa-647, and 405 nm for DAPI or Alexa-405.

Purification of BV and ODV and fractionation into envelope and nucleocapsid fractions. Sf9 cells (2.0×10^8) were infected with *vubi*KO-Myc-*vubi* virus at an MOI of 0.1, and cells were harvested at 7 days p.i. The infected cells were pelleted at 3,000 rpm to separate the medium containing BV and the cell pellet containing ODV. The BV-containing medium (90 ml) was centrifuged at 8,000 $\times$ *g* in a Beckman JA12 rotor to pellet cell debris. The BV in the cell debris-free supernatant was pelleted by centrifugation at 100,000 $\times$ *g* (21,000 rpm) in a Beckman SW28 rotor at 4°C. The pelleted BV was resuspended in 400 μl of 0.1$\times$ Tris-EDTA (TE) buffer with 1% protease inhibitor cocktail as described above. The resuspended BV was loaded onto a continuous sucrose density gradient (25 to 60%) and centrifuged at 100,000 $\times$ *g* (24,000 rpm) in a Beckman SW41 rotor at 4°C for 1.5 h. The BV band was collected and diluted with an equal volume of 0.1$\times$ TE. The diluted, purified BV was centrifuged at 100,000 $\times$ *g* (24,000 rpm) in a

Beckman SW41 rotor at 4°C for 30 min to pellet the BV. The purified BV protein concentration was determined by the Bradford assay (68).

The cell pellet containing occlusion bodies (OBs) was washed twice with 5 ml of sterile distilled water (dH_2O) to remove any trace medium. The cell pellet was resuspended in 2 ml of 2% (vol/vol) Triton X-100 and incubated at 37°C for 1 h. Following Triton X-100 treatment, the cells were treated with 2% deoxycholate at 37°C for 1 h. The material was then treated with 0.1% SDS and vortexed for 10 min. OBs were pelleted at 3,000 × *g* for 1 min and resuspended in 100 μl dH_2O. ODVs were released from OBs by incubation with alkaline dissolution buffer (0.002 M EDTA, 0.2 M Na_2CO_3, 0.34 M NaCl, pH 10.8) for 30 min. The dissolution of OBs was checked by microscopy. The reaction was neutralized with 20 μl 1.0 M Tris-HCl, pH 7.2. The remaining cell debris and insoluble material were pelleted for 5 min at 3,000 × *g*. ODVs in the supernatant were loaded onto a step sucrose gradient (30 to 60%). The gradient was centrifuged at 100,000 × *g* (24,000 rpm) in a Beckman SW41 rotor at 4°C for 90 min. The multiple ODV bands were collected and diluted with 2 volumes of 0.1× TE. The diluted ODV was pelleted by centrifugation at 55,000 × *g* (18,000 rpm) in a Beckman SW41 rotor at 4°C for 60 min. The purified ODV concentration was determined by Bradford assay.

Fractionation of BV and ODV into nucleocapsid and envelope fractions was performed as described previously (12, 69). Purified BV or ODV (250 μg) was incubated for 30 min at room temperature with 1% NP-40 in 10 mM Tris-HCl, pH 8.5, in a 250-μl reaction volume. NP-40-treated BV and ODV were layered onto 30% (wt/vol) glycerol cushions with 10 mM Tris-HCl, pH 8. The step gradient was centrifuged at 150,000 × *g* (34,000 rpm) in a Beckman SW60 rotor at 4°C for 1 h. The envelope fraction proteins from the top of the cushion were recovered by trichloroacetic acid (TCA) precipitation. The nucleocapsid pellets of BV and ODV were resuspended in 10 mM Tris-HCl, pH 7.4. For TCA protein precipitation, 25 volumes of 100% TCA stock was added to the protein sample and incubated at 4°C for 10 min. The protein precipitate was pelleted at 14,000 rpm for 5 min, followed by a cold acetone wash. After two washes with acetone, the pellet was dried at 95°C for 5 min to remove any residual acetone.

Mass spectrometric analysis and detection of viral and cellular ubiquitinated proteins. Purified BV or ODV or coimmunoprecipitated samples were analyzed by mass spectrometry at the University of British Columbia's Centre for High-Throughput Biology. The samples were loaded onto SDS-PAGE gels, and excised gel pieces were digested with trypsin followed by extraction. Experimental and control samples were differentially labeled with formaldehyde isotopologues, followed by liquid chromatography-tandem mass spectrometry (MS-MS) analysis. The MS-MS data were searched against databases created from proteins associated with Sf9 cells (http://www.ncbi.nlm.nih.gov/genome/?term=Sf9) and AcMNPV from UniProt using MaxQuant. To identify tryptic peptide, the MS data were analyzed with MASCOT (70). The C terminus of vUbi is Gly-Gly-Tyr, unlike that of cUbi, which is Gly-Gly. Normally, any amino acid extensions on ubiquitin-like proteins are cleaved to Gly-Gly by isopeptidase (71). However, to determine if vUbi was covalently linked to substrate proteins via Gly-Gly-Tyr linkage, the tryptic peptide MS data were analyzed with MASCOT (70). Tryptic peptides ubiquitinated by uncleaved vUbi would differ in molecular weight by a Tyr compared to Gly-Gly ubiquitination. The false-discovery rate that was used as a threshold for discovery was 1% at both the peptide and protein levels (70).

Western blot analysis. SDS-PAGE-separated proteins were electrotransferred onto Millipore Immobilon membranes using a Bio-Rad transfer apparatus as recommended in the manufacturer's protocol. The membranes were blocked for 1 h in blocking solution (5% skim milk in Tris-buffered saline and Tween 20 [TBST] [50 mM Tris, 150 mM NaCl, and 0.5% Tween 20]), followed by a 1-h incubation with the primary antibody. The following primary antibodies were used: mouse monoclonal anti-HA-horseradish peroxidase (HRP) (1:5,000; Invitrogen), mouse monoclonal anti-GP64-V5 (1:200), rabbit polyclonal anti-AC141 (1:2,500), mouse monoclonal anti-VP39 (1:3,000), mouse monoclonal anti-Myc (1:200; Santa Cruz), and mouse monoclonal anti-HA (1:1,000; Covance). The following secondary antibodies conjugated to horseradish peroxidase were used: rabbit anti-mouse (1:15,000) and goat anti-rabbit (1:15,000) (Jackson ImmunoResearch Laboratories Inc.). Bound antibodies were detected by incubation with peroxidase-conjugated secondary antibody and detected with the Western-Lightening Plus ECL enhanced-chemiluminescence system (Bio-Rad). Membranes were imaged with the Bio-Rad ChemiDoc MP imaging system. Relative band intensities were determined using Bio-Rad Image Lab v5.1 software.

ACKNOWLEDGMENTS

This study was supported in part by funding from the Natural Science and Engineering Research Council (D.A.T.).

We thank Michael Weis for assistance with confocal microscopy and Jason Rogalski of the University of British Columbia's Proteomics Core Facility for assistance with the proteomic analyses.

REFERENCES

1. Braunagel SC, Summers MD. 2007. Molecular biology of the baculovirus occlusion-derived virus envelope. Curr Drug Targets 8:1084–1095. https://doi.org/10.2174/138945007782151315.
2. Fang S, Weissman AM. 2004. A field guide to ubiquitylation. Cell Mol Life Sci 61:1546–1561. https://doi.org/10.1007/s00018-004-4129-5.
3. Komander D. 2009. The emerging complexity of protein ubiquitination. Biochem Soc Trans 37:937–953. https://doi.org/10.1042/BST0370937.
4. Swatek KN, Komander D. 2016. Ubiquitin modifications. Cell Res 26:399–422. https://doi.org/10.1038/cr.2016.39.
5. Deshaies RJ, Joazeiro CA. 2009. RING domain E3 ubiquitin ligases. Annu

Rev Biochem 78:399–434. https://doi.org/10.1146/annurev.biochem.78.101807.093809.
6. Jackson PK, Eldridge AG, Freed E, Furstenthal L, Hsu JY, Kaiser BK, Reimann JD. 2000. The lore of the RINGs: substrate recognition and catalysis by ubiquitin ligases. Trends Cell Biol 10:429–439. https://doi.org/10.1016/S0962-8924(00)01834-1.
7. Ardley HC, Robinson PA. 2005. E3 ubiquitin ligases. Essays Biochem 41:15–30.
8. Morreale FE, Walden H. 2016. Types of ubiquitin ligases. Cell 165:248–248.e1. https://doi.org/10.1016/j.cell.2016.03.003.
9. Randow F, Lehner PJ. 2009. Viral avoidance and exploitation of the ubiquitin system. Nat Cell Biol 11:527–534. https://doi.org/10.1038/ncb0509-527.
10. Gustin JK, Moses AV, Fruh K, Douglas JL. 2011. Viral takeover of the host ubiquitin system. Front Microbiol 2:161. https://doi.org/10.3389/fmicb.2011.00161.
11. Dai X, Stewart TM, Pathakamuri JA, Li Q, Theilmann DA. 2004. Autographa californica multiple nucleopolyhedrovirus exon0 (orf141), which encodes a RING finger protein, is required for efficient production of budded virus. J Virol 78:9633–9644. https://doi.org/10.1128/JVI.78.18.9633-9644.2004.
12. Fang M, Dai X, Theilmann DA. 2007. Autographa californica multiple nucleopolyhedrovirus EXON0 (ORF141) is required for efficient egress of nucleocapsids from the nucleus. J Virol 81:9859–9869. https://doi.org/10.1128/JVI.00588-07.
13. Fang M, Nie Y, Dai X, Theilmann DA. 2008. Identification of AcMNPV EXON0 (ac141) domains required for efficient production of budded virus, dimerization and association with BV/ODV-C42 and FP25. Virology 375:265–276. https://doi.org/10.1016/j.virol.2008.01.036.
14. Plechanovova A, Jaffray EG, Tatham MH, Naismith JH, Hay RT. 2012. Structure of a RING E3 ligase and ubiquitin-loaded E2 primed for catalysis. Nature 489:115–120. https://doi.org/10.1038/nature11376.
15. Pickart CM, Fushman D. 2004. Polyubiquitin chains: polymeric protein signals. Curr Opin Chem Biol 8:610–616. https://doi.org/10.1016/j.cbpa.2004.09.009.
16. Sadowski M, Suryadinata R, Tan AR, Roesley SN, Sarcevic B. 2012. Protein monoubiquitination and polyubiquitination generate structural diversity to control distinct biological processes. IUBMB Life 64:136–142. https://doi.org/10.1002/iub.589.
17. Guarino LA. 1990. Identification of a viral gene encoding a ubiquitin-like protein. Proc Natl Acad Sci U S A 87:409–413. https://doi.org/10.1073/pnas.87.1.409.
18. Reilly LM, Guarino LA. 1996. The viral ubiquitin gene of *Autographa californica* nuclear polyhedrosis virus is not essential for viral replication. Virology 218:243–247. https://doi.org/10.1006/viro.1996.0185.
19. Lin XA, Chen Y, Xu WH, Yi YZ, Zhang ZF. 2008. Characterization of the *Autographa californica* nucleopolyhedrovirus ubiquitin gene promoter. Z Naturforsch C 63:277–283. https://doi.org/10.1515/znc-2008-3-419.
20. Guarino LA, Smith G, Dong W. 1995. Ubiquitin is attached to membranes of baculovirus particles by a novel type of phospholipid anchor. Cell 80:301–309. https://doi.org/10.1016/0092-8674(95)90413-1.
21. Haas AL, Katzung DJ, Reback PM, Guarino LA. 1996. Functional characterization of the ubiquitin variant encoded by the baculovirus *Autographa californica*. Biochemistry 35:5385–5394. https://doi.org/10.1021/bi9524981.
22. Imai N, Matsuda N, Tanaka K, Nakano A, Matsumoto S, Kang W. 2003. Ubiquitin ligase activities of *Bombyx mori* nucleopolyhedrovirus RING finger proteins. J Virol 77:923–930. https://doi.org/10.1128/JVI.77.2.923-930.2003.
23. Green MC, Monser KP, Clem RJ. 2004. Ubiquitin protein ligase activity of the anti-apoptotic baculovirus protein Op-IAP3. Virus Res 105:89–96. https://doi.org/10.1016/j.virusres.2004.04.017.
24. Wu X, Stewart S, Theilmann DA. 1993. Alternative transcriptional initiation as a novel mechanism for regulating expression of a baculovirus trans activator. J Virol 67:5833–5842.
25. Yoo S, Guarino LA. 1994. The *Autographa californica* nuclear polyhedrosis virus ie2 gene encodes a transcriptional regulator. Virology 202:746–753. https://doi.org/10.1006/viro.1994.1396.
26. Ardisson-Araujo DM, Melo FL, Clem RJ, Wolff JL, Ribeiro BM. 2015. A betabaculovirus-encoded gp64 homolog codes for a functional envelope fusion protein. J Virol 90:1668–1672. https://doi.org/10.1128/JVI.02491-15.
27. Monsma SA, Oomens AG, Blissard GW. 1996. The GP64 envelope fusion protein is an essential baculovirus protein required for cell-to-cell transmission of infection. J Virol 70:4607–4616.
28. Oomens AG, Blissard GW. 1999. Requirement for GP64 to drive efficient budding of *Autographa californica* multicapsid nucleopolyhedrovirus. Virology 254:297–314. https://doi.org/10.1006/viro.1998.9523.
29. Fang M, Nie Y, Theilmann DA. 2009. AcMNPV EXON0 (AC141) which is required for the efficient egress of budded virus nucleocapsids interacts with beta-tubulin. Virology 385:496–504. https://doi.org/10.1016/j.virol.2008.12.023.
30. Marek M, Merten OW, Galibert L, Vlak JM, van Oers MM. 2011. Baculovirus VP80 protein and the F-actin cytoskeleton interact and connect the viral replication factory with the nuclear periphery. J Virol 85:5350–5362. https://doi.org/10.1128/JVI.00035-11.
31. Whitford M, Faulkner P. 1992. A structural polypeptide of the baculovirus *Autographa californica* nuclear polyhedrosis virus contains O-linked N-acetylglucosamine. J Virol 66:3324–3329.
32. Olszewski J, Miller LK. 1997. A role for baculovirus GP41 in budded virus production. Virology 233:292–301. https://doi.org/10.1006/viro.1997.8612.
33. Goley ED, Ohkawa T, Mancuso J, Woodruff JB, D'Alessio JA, Cande WZ, Volkman LE, Welch MD. 2006. Dynamic nuclear actin assembly by Arp2/3 complex and a baculovirus WASP-like protein. Science 314:464–467. https://doi.org/10.1126/science.1133348.
34. Vialard JE, Richardson CD. 1993. The 1,629-nucleotide open reading frame located downstream of the *Autographa californica* nuclear polyhedrosis virus polyhedrin gene encodes a nucleocapsid-associated phosphoprotein. J Virol 67:5859–5866.
35. Wang R, Deng F, Hou D, Zhao Y, Guo L, Wang H, Hu Z. 2010. Proteomics of the *Autographa californica* nucleopolyhedrovirus budded virions. J Virol 84:7233–7242. https://doi.org/10.1128/JVI.00040-10.
36. Ke J, Wang J, Deng R, Wang X. 2008. *Autographa californica* multiple nucleopolyhedrovirus ac66 is required for the efficient egress of nucleocapsids from the nucleus, general synthesis of preoccluded virions and occlusion body formation. Virology 374:421–431. https://doi.org/10.1016/j.virol.2007.12.033.
37. Callis J. 2014. The ubiquitination machinery of the ubiquitin system. Arabidopsis Book 12:e0174. https://doi.org/10.1199/tab.0174.
38. Reyes-Turcu FE, Ventii KH, Wilkinson KD. 2009. Regulation and cellular roles of ubiquitin-specific deubiquitinating enzymes. Annu Rev Biochem 78:363–397. https://doi.org/10.1146/annurev.biochem.78.082307.091526.
39. Ranaweera RS, Yang X. 2013. Auto-ubiquitination of Mdm2 enhances its substrate ubiquitin ligase activity. J Biol Chem 288:18939–18946. https://doi.org/10.1074/jbc.M113.454470.
40. Clegg HV, Itahana K, Zhang Y. 2008. Unlocking the Mdm2-p53 loop: ubiquitin is the key. Cell Cycle 7:287–292. https://doi.org/10.4161/cc.7.3.5358.
41. Chen A, Kleiman FE, Manley JL, Ouchi T, Pan ZQ. 2002. Autoubiquitination of the BRCA1*BARD1 RING ubiquitin ligase. J Biol Chem 277:22085–22092. https://doi.org/10.1074/jbc.M201252200.
42. Amemiya Y, Azmi P, Seth A. 2008. Autoubiquitination of BCA2 RING E3 ligase regulates its own stability and affects cell migration. Mol Cancer Res 6:1385–1396. https://doi.org/10.1158/1541-7786.MCR-08-0094.
43. Yamauchi K, Wada K, Tanji K, Tanaka M, Kamitani T. 2008. Ubiquitination of E3 ubiquitin ligase TRIM5 alpha and its potential role. FEBS J 275:1540–1555. https://doi.org/10.1111/j.1742-4658.2008.06313.x.
44. Clem RJ, Robson M, Miller LK. 1994. Influence of infection route on the infectivity of baculovirus mutants lacking the apoptosis-inhibiting gene p35 and the adjacent gene p94. J Virol 68:6759–6762.
45. Pruneda JN, Stoll KE, Bolton LJ, Brzovic PS, Klevit RE. 2011. Ubiquitin in motion: structural studies of the ubiquitin-conjugating enzyme approximately ubiquitin conjugate. Biochemistry 50:1624–1633. https://doi.org/10.1021/bi101913m.
46. Reyes-Turcu FE, Horton JR, Mullally JE, Heroux A, Cheng X, Wilkinson KD. 2006. The ubiquitin binding domain ZnF UBP recognizes the C-terminal diglycine motif of unanchored ubiquitin. Cell 124:1197–1208. https://doi.org/10.1016/j.cell.2006.02.038.
47. Hurley JH, Lee S, Prag G. 2006. Ubiquitin-binding domains. Biochem J 399:361–372. https://doi.org/10.1042/BJ20061138.
48. Sette P, Nagashima K, Piper RC, Bouamr F. 2013. Ubiquitin conjugation to Gag is essential for ESCRT-mediated HIV-1 budding. Retrovirology 10:79. https://doi.org/10.1186/1742-4690-10-79.
49. Li Z, Blissard GW. 2012. Cellular VPS4 is required for efficient entry and egress of budded virions of *Autographa californica* multiple nucleopolyhedrovirus. J Virol 86:459–472. https://doi.org/10.1128/JVI.06049-11.
50. Rosinski M, Reid S, Nielsen LK. 2002. Kinetics of baculovirus replication and release using real-time quantitative polymerase chain reaction. Biotechnol Bioeng 77:476–480. https://doi.org/10.1002/bit.10126.

51. Luxton GW, Lee JI, Haverlock-Moyns S, Schober JM, Smith GA. 2006. The pseudorabies virus VP1/2 tegument protein is required for intracellular capsid transport. J Virol 80:201–209. https://doi.org/10.1128/JVI.80.1.201-209.2006.
52. Leelawong M, Lee JI, Smith GA. 2012. Nuclear egress of pseudorabies virus capsids is enhanced by a subspecies of the large tegument protein that is lost upon cytoplasmic maturation. J Virol 86:6303–6314. https://doi.org/10.1128/JVI.07051-11.
53. Huffmaster NJ, Sollars PJ, Richards AL, Pickard GE, Smith GA. 2015. Dynamic ubiquitination drives herpesvirus neuroinvasion. Proc Natl Acad Sci U S A 112:12818–12823. https://doi.org/10.1073/pnas.1512559112.
54. Mettenleiter TC. 2002. Herpesvirus assembly and egress. J Virol 76:1537–1547. https://doi.org/10.1128/JVI.76.4.1537-1547.2002.
55. Johnson DC, Baines JD. 2011. Herpesviruses remodel host membranes for virus egress. Nat Rev Microbiol 9:382–394. https://doi.org/10.1038/nrmicro2559.
56. Lee CP, Liu GT, Kung HN, Liu PT, Liao YT, Chow LP, Chang LS, Chang YH, Chang CW, Shu WC, Angers A, Farina A, Lin SF, Tsai CH, Bouamr F, Chen MR. 2016. The ubiquitin ligase Itch and ubiquitination regulate BFRF1-mediated nuclear envelope modification for Epstein-Barr virus maturation. J Virol 90:8994–9007. https://doi.org/10.1128/JVI.01235-16.
57. Granados RR, Lawler KA. 1981. In vivo pathway of *Autographa californica* baculovirus invasion and infection. Virology 108:297–308. https://doi.org/10.1016/0042-6822(81)90438-4.
58. Guo Y, Yue Q, Gao J, Wang Z, Chen YR, Blissard GW, Liu TX, Li Z. 2017. Roles of cellular NSF protein in entry and nuclear egress of budded virions of Autographa californica multiple nucleopolyhedrovirus. J Virol 91:01111-17. https://doi.org/10.1128/JVI.01111-17.
59. Hatsell S, Cowin P. 2001. Deconstructing desmoplakin. Nat Cell Biol 3:E270–E272. https://doi.org/10.1038/ncb1201-e270.
60. Sumigray KD, Lechler T. 2011. Control of cortical microtubule organization and desmosome stability by centrosomal proteins. Bioarchitecture 1:221–224. https://doi.org/10.4161/bioa.18403.
61. Biswas S, Blissard GW, Theilmann DA. 2016. *Trichoplusia ni* kinesin-1 associates with AcMNPV nucleocapsid proteins and is required for the production of budded virus. J Virol 90:3480–3495. https://doi.org/10.1128/JVI.02912-15.
62. Luckow VA, Lee SC, Barry GF, Olins PO. 1993. Efficient generation of infectious recombinant baculoviruses by site-specific transposon-mediated insertion of foreign genes into a baculovirus genome propagated in *Escherichia coli*. J Virol 67:4566–4579.
63. Guarino LA, Smith MW. 1990. Nucleotide sequence and characterization of the 39K gene region of *Autographa californica* nuclear polyhedrosis virus. Virology 179:1–8. https://doi.org/10.1016/0042-6822(90)90266-T.
64. Datsenko KA, Wanner BL. 2000. One-step inactivation of chromosomal genes in Escherichia coli K-12 using PCR products. Proc Natl Acad Sci U S A 97:6640–6645. https://doi.org/10.1073/pnas.120163297.
65. Lung OY, Cruz-Alvarez M, Blissard GW. 2003. Ac23, an envelope fusion protein homolog in the baculovirus *Autographa californica* multicapsid nucleopolyhedrovirus, is a viral pathogenicity factor. J Virol 77:328–339. https://doi.org/10.1128/JVI.77.1.328-339.2003.
66. Ellison MJ, Hochstrasser M. 1991. Epitope-tagged ubiquitin. A new probe for analyzing ubiquitin function. J Biol Chem 266:21150–21157.
67. Javed MA, Biswas S, Willis LG, Harris S, Pritchard C, van Oers MM, Donly BC, Erlandson MA, Hegedus DD, Theilmann DA. 2017. *Autographa californica* multiple nucleopolyhedrovirus AC83 is a per os infectivity factor (PIF) protein required for occlusion-derived virus (ODV) and budded virus nucleocapsid assembly as well as assembly of the PIF complex in ODV envelopes. J Virol 91:e02115-16. https://doi.org/10.1128/JVI.02115-16.
68. Bradford MM. 1976. A rapid and sensitive method for the quantitation of microgram quantities of protein utilizing the principle of protein-dye binding. Anal Biochem 72:248–254. https://doi.org/10.1016/0003-2697(76)90527-3.
69. Braunagel SC, Summers MD. 1994. *Autographa californica* nuclear polyhedrosis virus, PDV, and ECV viral envelopes and nucleocapsids: structural proteins, antigens, lipid and fatty acid profiles. Virology 202:315–328. https://doi.org/10.1006/viro.1994.1348.
70. Perkins DN, Pappin DJ, Creasy DM, Cottrell JS. 1999. Probability-based protein identification by searching sequence databases using mass spectrometry data. Electrophoresis 20:3551–3567. https://doi.org/10.1002/(SICI)1522-2683(19991201)20:18<3551::AID-ELPS3551>3.0.CO;2-2.
71. Xu G, Jaffrey SR. 2013. Proteomic identification of protein ubiquitination events. Biotechnol Genet Eng Rev 29:73–109. https://doi.org/10.1080/02648725.2013.801232.
72. Hou D, Zhang L, Deng F, Fang W, Wang R, Liu X, Guo L, Rayner S, Chen X, Wang H, Hu Z. 2013. Comparative proteomics reveal fundamental structural and functional differences between the two progeny phenotypes of a baculovirus. J Virol 87:829–839. https://doi.org/10.1128/JVI.02329-12.
73. Katsuma S, Kokusho R. 2017. A conserved glycine residue is required for proper functioning of a baculovirus VP39 protein. J Virol 91:e02253-16. https://doi.org/10.1128/JVI.02253-16.
74. McCarthy CB, Dai X, Donly C, Theilmann DA. 2008. Autographa californica multiple nucleopolyhedrovirus ac142, a core gene that is essential for BV production and ODV envelopment. Virology 372:325–339. https://doi.org/10.1016/j.virol.2007.10.019.
75. Li K, Wang Y, Bai H, Wang Q, Song J, Zhou Y, Wu C, Chen X. 2010. The putative pocket protein binding site of *Autographa californica* nucleopolyhedrovirus BV/ODV-C42 is required for virus-induced nuclear actin polymerization. J Virol 84:7857–7868. https://doi.org/10.1128/JVI.00174-10.
76. Theilmann DA, Stewart S. 1991. Identification and characterization of the IE-1 gene of Orgyia pseudotsugata multicapsid nuclear polyhedrosis virus. Virology 180:492–508. https://doi.org/10.1016/0042-6822(91)90063-H.
77. Gong Y, Li Z, Wang L, Pan L, Yang K, Pang Y. 2003. Characterization of bro-b gene of Spodoptera litura multicapsid nucleopolyhedrovirus. Virus Genes 27:115–123. https://doi.org/10.1023/A:1025773324560.
78. Cheng X, Krell P, Arif B. 2001. P34.8 (GP37) is not essential for baculovirus replication. J Gen Virol 82:299–305. https://doi.org/10.1099/0022-1317-82-2-299.
79. Wang Y, Wang Q, Liang C, Song J, Li N, Shi H, Chen X. 2008. *Autographa californica* multiple nucleopolyhedrovirus nucleocapsid protein BV/ODV-C42 mediates the nuclear entry of P78/83. J Virol 82:4554–4561. https://doi.org/10.1128/JVI.02510-07.
80. McDougal VV, Guarino LA. 2000. The *Autographa californica* nuclear polyhedrosis virus p143 gene encodes a DNA helicase. J Virol 74:5273–5279. https://doi.org/10.1128/JVI.74.11.5273-5279.2000.
81. Nie Y, Fang M, Erlandson MA, Theilmann DA. 2012. Analysis of the autographa californica multiple nucleopolyhedrovirus overlapping gene pair lef3 and ac68 reveals that AC68 is a per os infectivity factor and that LEF3 is critical, but not essential, for virus replication. J Virol 86:3985–3994. https://doi.org/10.1128/JVI.06849-11.